AIChE

Advancement of Fischer-Tropsch Synthesis via Utilization of Supercritical Fluid Reaction Media

Nimir O. Elbashir and Dragomir B. Bukur
Chemical Engineering Program, Texas A&M University at Qatar, Education City, P.O. Box 23874, Doha, Qatar

Ed Durham and Christopher B. Roberts
Dept. of Chemical Engineering, Ross Hall, Auburn University, AL 36849

DOI 10.1002/aic.12032
Published online October 1, 2009 in Wiley InterScience (www.interscience.wiley.com).

The Fischer Tropsch Synthesis (FTS) reaction has been studied and for nearly a century for the production of fuels and chemicals from nonpetroleum sources. Research and utilization have occurred in both gas phase (fixed bed) and liquid phase (slurry bed) operation. The use of supercritical fluids as the reaction media for FTS (SCF-FTS) now has a 20-year history. Although a great deal of progress in SCF-FTS has been made on the lab scale, this process has yet to be expanded to pilot or industrial scale. This article reviews the research activities involving supercritical FTS and published in open literature from 1989 to 2008. © 2009 American Institute of Chemical Engineers *AIChE J,* 56: 997–1015, 2010
Keywords: Fischer-Tropsch synthesis, supercritical fluids, reaction engineering, cobalt catalyst, iron catalyst, ruthenium catalyst

Introduction to supercritical fluids for catalysis

The concept of using supercritical fluids (SCFs) as solvents has been in circulation since their discovery in the nineteenth century.[1] Industrial utilization of SCFs has received considerable attention since the early 1980s, starting with the development of technologies for extraction of commodity chemicals and fuels.[2] By the mid 1980s, research on new applications of SCFs shifted toward more complex and valuable substances that undergo a much broader range of physical and chemical transformations.[2] A great deal of research activities have taken place in studies of reactions, separations, and materials processing of polymers, foods, surfactants, pharmaceuticals, and hazardous wastes.[3] SCFs are recognized as a unique medium for chemical reactions, offering single phase operation, a density that is sufficient to afford substantial dissolution power, a higher diffusivity, and lower viscosity than in liquids. These properties can result in significant enhancement of mass transfer and/or heat transfer. Additionally, conducting chemical reactions at near-critical conditions affords excellent opportunities to tune the reaction environment (solvent properties) through modest changes in temperature and pressure. These properties can help to eliminate transport limitations on reaction rates, integrate reaction and product separation processes,[4] and enhance in situ extraction of low volatility products (e.g., heavy hydrocarbons) from porous catalysts.[5]

The main areas of heterogeneously catalyzed hydrogenation reactions were classified by Hyde et al.[6] according to the following categories: (1) the hydrogenation of food compounds such as fatty acids or oils to produce higher value derivatives; (2) the formation of precursor building blocks for pharmaceuticals and fine chemicals, and (3) asymmetric hydrogenation. In their book, McHugh and Krukonis,[2] address the uniqueness of applying a supercritical medium to many of the above classes of heterogeneous reactions, as well as to homogenous reactions such as selective oxidations, hydrogenations, hydroformylations, alkylations, and

Correspondence concerning this article should be addressed to N. O. Elbashir at nelbashir@tamu.edu

polymerizations. In another review article, Subramaniam[5] addressed many of the advantages of using SCF as a reaction medium in heterogeneous catalysis relative to conventional media (gas and liquid phase reactions), emphasizing the ability of the SCF media to extract low volatile hydrocarbons from porous catalysts in situ. This extraction increases pore accessibilities, enhances catalyst stability to coking, and increases primary product selectivity. Coke formation inside catalyst pores normally results in a drop in activity and eventually leads to complete deactivation of the catalyst. Coke formation inside the catalyst pores is controlled by many factors, including reaction temperature, reaction pressure, acidity, and catalyst structure.[7] To stabilize the catalyst activity, the rate of coke formation should be minimized by maximizing the rate at which coke precursors are removed, preventing them from being converted to coke inside the catalyst pores. Effective in situ removal of the coke precursors by a near-critical reaction medium has also been demonstrated by Subramaniam.[5] The liquid-like density and gas-like transport properties offer a superior medium to mitigate coke buildup and, therefore, alleviate pore diffusion limitations.

Baiker[4] demonstrated that the various steps in heterogeneous catalysis (transport of reactants to the gas–liquid interface, adsorption, internal and external diffusion, chemical reaction, and desorption) can all be directly or indirectly affected by pressure. This is particularly true in going from near-critical to supercritical conditions, providing an opportunity to better control the rate and selectivity of heterogeneously catalyzed reactions. In particular, Baiker[4] discussed the reduction of mass transfer resistances through the elimination of the gas–liquid interface.

SCFs also offer unique media for conducting heterogeneous reactions in a continuous mode in dense media. Thomas Swan Co. Ltd[8] claimed to have designed one of the first continuous high-pressure reactors for both pilot and commercial scale production. Their design is claimed to be highly flexible and can be used for up to 1000 tons per annum for fine chemical synthesis in SC-CO_2.[6]

Other comprehensive reviews of utilization of supercritical fluids in homogeneous and heterogeneous chemical reactions can be found in Savage et al.[9] and Satio.[10] Heterogeneous reactions were reviewed by Baiker,[4] Hyde et al.,[6] Subramaniam,[5,11] and Jessop and Leitner.[12] More recently, Seki et al.[13] wrote a review article covering applications of SCFs in heterogeneous catalytic hydrogenation of organic compounds, concluded that SCFs (particularly CO_2) offer attractive opportunities as substitutes for classical organic solvents.

Introduction to Fischer Tropsch synthesis

Fischer-Tropsch Synthesis (FTS) is a mature process for the production of hydrocarbons from syngas ($CO + H_2$). The hydrocarbons are of varying lengths (methane to hard wax) and types (n-alkanes, n-alkenes (primarily terminal), branched compounds (primarily mono-methyl), and oxygenates (alcohols, ketones, aldehydes, and acids)).[14,15] The syngas can be generated from any carbonaceous material (coal, natural gas, biomass, etc).[16] FTS diesel has a higher cetane index and is cleaner burning than petro-diesel, emitting lower SO_x (FTS requires the syngas to be sulfur free,[17] resulting in a sulfur-free product), fewer NOx, less CO, and lower particulates.[18]

There are two modes of Fischer Tropsch operation used industrially: high temperature (HTFT) and low temperature (LTFT).[19] HTFT utilizes a fused iron catalyst in a fluidized bed reactor for the production of light olefins and gasoline.[20] LTFT utilizes either a precipitated iron or supported cobalt catalyst (ruthenium can be used for LTFT, but its cost and availability disqualify it from industrial use[19]) in either a fixed bed (gas phase) or slurry (liquid phase) reactor for the production of diesel and wax.[21]

The use of supercritical fluids in FTS (SCF-FTS) has been focused almost exclusively on LTFT. Consequently, this review will be limited to that mode of operation.

Sasol's original LTFT reactor design utilized a fixed catalyst bed. The reactor is a downflow vertical shell and tube system 5-cm ID, 12-m long tubes in a 3-m shell (steam is generated in the shell).[22] At a temperature of 230°C and a pressure of 27 bar, these reactors have a capacity of 500 barrel per day (BPD).[22] The high number of narrow tubes is necessitated by the amount of heat released by the reaction[23]:

$$CO + 2H_2 \rightarrow (CH_2) + H_2O + 146\ \text{kJ}$$

where CH_2 is the building block for the propagation process.

This design results in a high pressure drop (3–7 bar),[21] that when combined with high recycle rates, produces high compression costs. Thermal nonuniformity in the fixed-bed reactor suppresses average temperature, increasing the catalyst loading required for a given production rate. The high number of tubes gives poor economies of scale and the fixed bed design necessitates shutting down the reactor to replace the catalyst. As a result, reactor down-time, labor intensive turnarounds, and difficulty in maintaining system activity and selectivity are issues with fixed bed operation.[24]

To overcome these problems, Sasol developed a slurry-bed FTS reactor with a liquid phase reaction media (using produced wax as the media thereby giving a much higher thermal mass than gas phase).[24] The pressure drop approaches the hydraulic head of the slurry, resulting in lower compression costs. The reactor behaves much like a continuous stirred tank reactor (CSTR), giving superior temperature uniformity. This allows for higher catalyst activity and superior selectivity control. Additionally, the slurry reactor system is far cheaper than the fixed bed equivalent (more than 60% less) and the capacity for online catalyst removal lessens the need for costly turn-around. The primary challenges facing slurry reactor technology are the separation of the solid catalyst from the heavy liquid product[24] and catalyst attrition.[25]

Because the catalyst particles are smaller in a slurry bed reactor than in a fixed bed reactor, the slurry reactor gives higher production per unit mass of catalyst. The slurry-phase FTS also gives superior selectivity including reduced methane formation,[14] enhanced olefin selectivity,[24] and enhanced wax selectivity.[14]

Concerns about the price and availability of crude oil and political stability have created a great deal of recent industrial and political interest in Fischer Tropsch Synthesis to

Table 1. Critical Properties of Hydrocarbon Solvents Used in SCF-FTS Compared to the Critical Properties of Common SCFs CO_2 and Water

Solvent	Critical Temp., T_c (°C)	Critical Pressure, P_c (bar)	Critical Density, ρ_c (g/cm^3)
Carbon dioxide	30.9	73.75	
Water	373.9	220.6	
Propane (C_3H_8)	96.6	42.5	0.224
n-Butane (C_4H_{10})	151.6	38.0	0.227
n-Pentane (C_5H_{12})	196.7	33.6	0.232
n-Hexane (C_6H_{14})	233.3	29.7	0.233
n-Heptane (C_7H_{16})	266.6	27.8	0.235
n-Decane ($C_{10}H_{22}$)	344.8	21.1	0.229

Data obtained from *NIST Scientific and Database* website: http://webbook.nist.gov/chemistry/name-ser.html.

utilize stranded natural gas and coal. However, the rate of CO_2 generation in the overall process from these feedstocks represents another hurdle for the implementation of XTL (X = G for natural gas as source of syngas, X = C for coal as source of syngas, and X = B for biomass as source of syngas). The hope of carbon neutrality and of a greater utilization of biomass has enhanced interest in BTL specifically, and FTS in general,[26] for alternative fuels technologies. This review discusses the potential of supercritical fluid FTS technology as an option in XTL processes.

Supercritical fluid solvent media for FTS

In spite of the above advantages for liquid phase (slurry bed) FTS, the simplicity of fixed-bed operation is desirable, especially for operation on a smaller scale. That fixed bed operation has certain advantages is evidenced by Shell's choice to use a fixed bed reactor for their FTS operations (SMDS).[22] The desire to combine the advantages of slurry bed FTS with the simplicity of fixed bed operation has motivated research into the application of supercritical fluid solvents to improve the catalyst activity and selectivity. Conducting FTS under supercritical fluid (SCF) solvent conditions (SCF-FTS) affords unique opportunities to manipulate the reaction environment by means of the tunable physicochemical properties of the supercritical phase (e.g., gas-like diffusivity and liquid-like heat transfer and solubilities) that created opportunities to improve FTS process performance and economics.

Previous investigations into SCF-FTS have suggested the following advantages: (1) in situ extraction of heavy hydrocarbons from the catalyst resulting due to high solubility in the supercritical phase (e.g., Refs. 27–30); (2) elimination of interphase transport limitations, thus promoting reaction pathways toward the desired products (e.g., Ref. 29); (3) enhanced desorption of primary products prior to their undergoing secondary reactions promotes a high α-olefin selectivity[27,30,32–35]; and (4) superior heat transfer compared to gas-phase reaction, resulting in more long chain products (e.g., Refs. 27, 28, and 35).

Fujimoto's group[36,37] first developed SCF-FTS and proposed the following selection criteria for the media:

(1) The media critical temperature and pressure are slightly lower than the typical reaction temperature and pressure.

(2) The media should not poison the catalysts and should be stable under the reaction conditions.

(3) The media should have a high affinity for aliphatic hydrocarbons to extract wax from the catalyst surface and reactor.

Given that LTFT typically operates at a temperature of 220 to 250°C,[22] this selection criteria sets pentane and hexane as logical choices for SCF-FTS media based on the critical properties shown in Table 1. As such, these hydrocarbon solvents are preferred over the common supercritical solvents of CO_2 and H_2O for FTS. In addition, high water content can poison supported cobalt catalysts,[38] and neither CO_2 nor water are inert with an iron catalyst (iron FT catalysts) are active toward the water gas shift reaction.[19] Hydrocarbons that have been investigated to date as supercritical solvents for SCF-FTS investigations include propane, *n*-pentane, *n*-hexane and hexanes, *n*-heptane and *n*-decane, while hexane is perhaps most commonly used. As saturated hydrocarbons are inert and are not coke precursors[27] under FTS conditions, they meet the second criteria. Sasol determined that the conversion and carbon number distribution from their fixed-bed reactors are independent of pressure (at a constant gas velocity), so they operate the reactors at a high pressure (27 to 45 bar).[22] This puts the critical pressure of pentane and hexane somewhat low, especially given that the total pressure in supercritical operation is the sum of the partial pressures of the reactants, products, and media. The third criterion is met with the hydrocarbon solvents given that they show high solubilities for other hydrocarbons. Consequently, work in SCF-FTS has focused almost exclusively on light hydrocarbon solvents. Figure 1 presents the density of *n*-hexane and *n*-pentane as function of pressure along different isotherms, illustrating the tunable physicochemical properties of these solvents near their critical point.

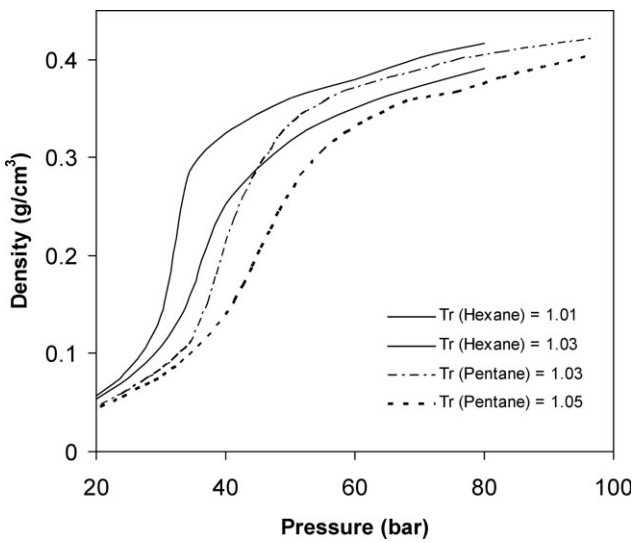

Figure 1. Plot of solvent density as function of pressure along various isotherms near the critical temperature for hexane and pentane solvents.

Densities calculated using Peng-Robinson equation of state.[39]

Investigations of Supercritical Phase Fischer Tropsch Synthesis

Overview

The pioneering study in SCF-FTS was performed by Yokota and Fujimoto (University of Tokyo, Japan) and was first reported in a short communication in 1989.[36] In a subsequent report, they compared the performance of the FTS reaction under supercritical phase conditions (hexane) in a fixed bed reactor to FTS performed under gas-phase (nitrogen media) and liquid-phase (hexadecane media) in a fixed bed reactor.[28] They demonstrated that conducting FTS reactions using SCF media offers unique characteristics, such as high diffusivity of reactant gases, effective removal of reaction heat, and in situ extraction of high molecular weight hydrocarbons (wax). Fujimoto's research group has since reported on several studies involving SCF-FTS including investigations of the influence of the catalyst type and characteristics (e.g., Refs. 40 and 41), selective synthesis of wax and heavy hydrocarbons (e.g., Refs. 42–44), and the influence of the type of solvent on the reaction performance (e.g., Refs. 36 and 37). Bukur and coworkers reported an enhancement in α-olefin selectivity during FTS reaction in SCF media on an iron catalyst.[32,34,45] Their results showed that the total olefin and 2-olefin selectivities were essentially independent of reaction temperature (at comparable conversion) but changed significantly when conditions were adjusted from conventional gas-phase operation to supercritical operation. Bochniak and Subramaniam[29] studied the influence of pressure on the SCF-FTS process, particularly its effect on the catalyst effectiveness factor and pore diffusivity. Davis and his coworkers[27,46] addressed the issue of catalyst stability in SCF-FTS reaction over a 25% Co/Al_2O_3 catalyst. Roberts and his coworkers have explored the advantages of SCF-FTS reaction over both alumina supported cobalt catalysts (15% $Co\text{-}Pt/Al_2O_3$ and 15% Co/Al_2O_3) and silica supported cobalt catalysts (15% Co/SiO_2 (high and low surface area silica support)).[35,39,47,48]

Researchers from the Institute of Coal Chemistry in China have also contributed to this field by exploring selective synthesis of heavier hydrocarbons from syngas on cobalt catalysts under SCF-FTS conditions.[49] Another group from Fundan University in Shanghai has reported enhancement of syngas diffusion in supercritical fluids.[50] Very recently, a group from Tarbiat Modares University in Tehran[51] as well as another group from Zheijang University of Technology[52] reported several improvements in catalyst activity and selectivity performance when operating the reaction under supercritical phase FTS conditions.

Several investigations have been made into the critical properties and phase behavior of SCF-FTS reaction mixtures: solvent-reactant mixtures,[53] solvent-product mixtures,[54,55] and solvent-reactant-products mixtures,[47] and thermodynamic modeling of FTS reaction mixtures.[56]

Effects of solvents, solvent mixtures, and phase behavior in SCF-FTS

Jacobs et al.[27] suggested that using a solvent mixture composed of 55 vol % hexane/45 vol % pentane should give favorable liquid-like densities, while still maintaining gas-like transport properties at a pressure of ~82.4 bar. They used a Hysys 2.1 process simulator for the determination of the critical properties of this solvent mixture and the effect of pressure on its density. Fan and Fujimoto[37] reported SCF-FTS performance in both hexane and pentane environments. They concluded that operating FTS reaction in supercritical pentane is preferred for wax synthesis experiments where the reaction temperature is low, while hexane is preferred for the production of light hydrocarbons and middle distillates (which require a higher reaction temperature). Fujimoto's group studied FTS performance in *n*-pentane, *n*-hexane, *n*-heptane, and *n*-octane[57] and found that the α-olefin selectivity of the produced hydrocarbons in *n*-pentane and *n*-hexane were similar and slightly lower than that in *n*-heptane, but notably higher than that in *n*-decane (see Figure 2). These results indicated that the extraction capacity of *n*-decane for α-olefins, one of the primary products of FTS, is lower than that of *n*-pentane, *n*-hexane, and *n*-heptane. The authors mentioned that *n*-decane was far from the critical point at the test conditions, which might result in the lower α-olefin selectivity.[57] In a recent study, Linhghu and Fujimoto conducted SCF-FTS experiments with several mixed solvents including a mixture of *n*-hexane and *n*-decane.[58] Their findings showed that a binary solvent composed of 75% *n*-hexane + 25% *n*-decane yielded an activity comparable with that obtained in an *n*-pentane + *n*-hexane solvent, however the *n*-hexane + *n*-decane solvent system gave considerably higher selectivity toward α-olefins and higher chain growth probability (α-value) when compared at similar conversion. They attributed these results to the higher affinity of *n*-decane to α-olefins that results in higher extraction ability of products from catalyst pores.[57]

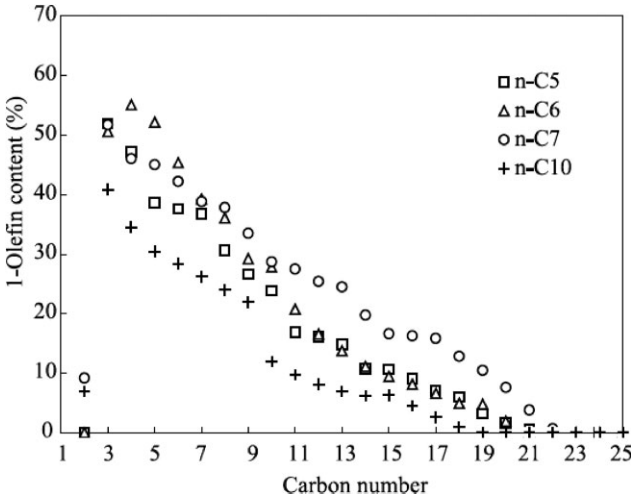

Figure 2. Effect of solvent on α-olefin content of hydrocarbons.

Reaction conditions: $T = 240°C$, $P_{total} = 4.5$ MPa, $P_{solvent} = 3.5$ MPa, and $W/F = 5$ g h/mol over a SiO_2 supported cobalt catalyst in a fixed bed reactor.[57]

Huang et al.[39] reported a comparison between the performance of FTS reaction in supercritical pentane and supercritical hexanes (over an alumina supported cobalt-catalyst and under similar reaction temperatures and densities). To achieve the same fluid density at 240°C ($\rho \approx 0.33$ g/cm^3),

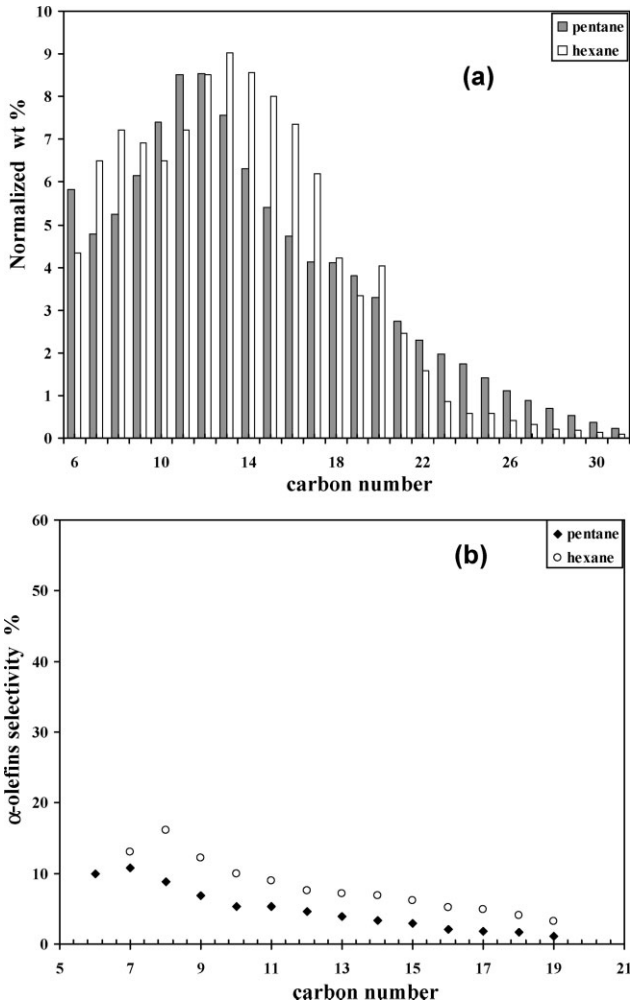

Figure 3. Hydrocarbon selectivity (a) normalized weight percentage vs. carbon number, and (b) α-olefin selectivity at constant medium solvent density ($\rho_{solvent}$ = 0.335 g/cm^3) in supercritical pentane and hexane phase FTS.

Pentane: 240°C, 65 bar, flow rate of 1 ml/min, and CO conversion of 92%. Hexane: 240°C, 38 bar, flow rate of 1 ml/min, and CO conversion: 61%. For both cases, a syngas flow rate of 50 sccm/g_{cat}; and H_2/CO ratio of 2.0 were used.[39]

the use of higher pressure was required in pentane (38 bar in hexane vs. 65 bar in pentane). The results presented in Figure 3 demonstrate that there is not much difference in the lumped hydrocarbon distributions for carbon numbers less than C_{20} in either supercritical pentane (Sc-pentane) or supercritical hexane (Sc-hexane) at constant density. Nevertheless, a higher CO conversion of 92% was observed in Sc-pentane FTS as opposed to 61% in Sc-hexane FTS, which was attributed to the influence of pressure on the reaction kinetics. It is noteworthy to mention that there was difference in α-olefin selectivity obtained in the two solvents; however, this can be attributed to the difference in CO conversion.[39]

Few studies have dealt with the phase behavior of the reaction mixture in SCF-FTS.[47,53–56] Joyce and his coworkers[55] studied the vapor–liquid equilibrium composition for a mixture of hexane (supercritical solvent) + C_{16} (representative heavy compound) at three different temperatures (199, 252, and 300°C). Addition of hexadecane and hexadecene (C_{16} hydrocarbons) to hexane solvent has been used to simulate the changes in the phase behavior as the percentage of heavy hydrocarbons in the product stream increases. Their findings showed that for 0.0326 mole fraction of C_{16} in the hexane + hexadecane mixture, the critical pressure and temperature of the mixture are 33.76 bar and 252°C, respectively. This represents a significant change in the critical properties from the pure hexane solvent critical properties of 32.4 bar, and 234.5°C, respectively. In another study, Gao et al.[53] reported critical points for hexane (>94 mole %) + reactant (CO and H_2) mixtures at different mole ratios. They observed that the critical temperature and critical density of the solvent-reactant mixture decreases as the concentration of CO and H_2 increases, whereby the critical pressure increases with CO and H_2 concentration. In another study, Polishuk et al.[56] compared the ability of two semipredictive thermodynamic models, namely the global phase diagram approach (GPDA) and the predictive Soave-Redlich-Kwong (PSRK), in describing the experimental phase behavior of binary homologous series of *n*-alkanes that represent FTS product spectrum. For a symmetric system of *n*-hexane + *n*-tetracosane, they found that the GPDA predicts very accurately the experimentally measured values of Joyce et al.[54] over a wide range of temperature, while PSRK significantly overestimates the bubble-point data.

Elbashir and Roberts[47] were the first to report experimental measurements of the critical point of a typical product stream from a supercritical phase FTS reaction mixture. This was performed by directly trapping the outlet stream from a fixed-bed FTS reactor (utilizing a cobalt-based catalyst) in a high pressure variable-volume-view cell at the reactor temperature and pressure. The variable-volume-view cell was then used to measure the critical properties of this FTS outlet stream which was composed of unreacted syngas, supercritical solvent (hexanes), and hydrocarbon products up to C_{30}. Their findings showed that the critical properties of this actual FTS reaction mixture are quite different from that of the pure supercritical solvent, resulting in different temperature, pressure, and composition requirements necessary to reach the desired single phase supercritical regime (as shown in Figure 4). As such, there is still a need for in depth studies on the phase behavior of supercritical phase FTS reaction mixtures (including the phase space location of single phase regions, multiphase regions, and the critical point loci) and how this changes or transitions from the reactor bed entrance (where there is only solvent and syngas present) through the catalyst bed whereby the presence of solid particles with extremely high heat capacities in addition to the presence of synthesized hydrocarbons may drastically change the phase behavior of the reaction mixture.

As would logically follow from the preceding discussion, an important consideration in SCF-FTS is the ratio of solvent to syngas used in the system. The higher this ratio, the closer the phase behavior and underlying physical properties of the mixture will resemble that of the solvent and the easier it will be to maintain single phase operation. However, to maintain the syngas partial pressure and reactor productivity, higher pressures and higher solvent throughput will be

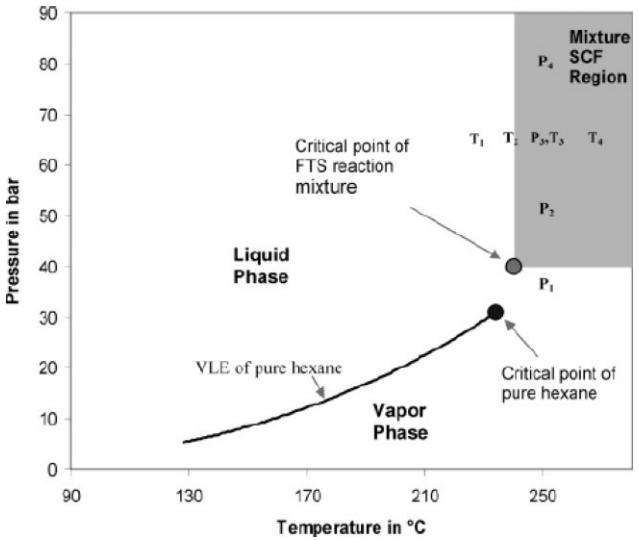

Figure 4. Critical point loci of a FTS reaction mixture composed of hexane 75 mol %, syngas (CO and H_2) 5 mol %, hydrocarbons, and water (20%) as measured using a high pressure variable volume view cell apparatus.[47]

needed. Elbashir et al.[48] investigated the influence of the hexane to syngas molar ratio on activity, the methane selectivity, and the probability to produce heavy hydrocarbons in SCF-FTS on a 15% Co/SiO_2 catalyst. As the hexane to syngas molar ratio increased, the CO conversion and methane selectivity decreased while the selectivity toward heavy products increased, pointing to another trade off in the determination of an appropriate solvent to syngas ratio in SCF-FTS. A molar ratio of 3.5 (media to syngas) is common in Fujimoto's work.

Improvements in catalyst activity and selectivity in SCF-FTS

Effects of SCF-FTS on Syngas Conversion. The seminal study in the field[36] reported a comparison between the FTS performance of a cobalt-based catalyst in each of the three phases (gas-phase, supercritical phase, and liquid phase) in a fixed bed reactor. Their findings demonstrated that the CO conversion in SCF-FTS was intermediate between the liquid phase reaction and the gas phase reaction. They explained this in terms of differences in diffusion rates of synthesis gas in different reaction media. Yokota et al.[28] proposed a model that described desorption and diffusion of FTS products in the three phases, indicating similarities between the supercritical phase and liquid-phase (see Figure 5). In general, diffusion rates are much faster in the supercritical phase than in the liquid phase but slower than in the gas phase. Bukur et al.[45] showed that SCF-FTS gave a conversion virtually identical to gas phase FTS and much higher than slurry-phase FTS. Fujimoto's group (Yakota and Fujimoto[59]) demonstrated that the activation energy for the various media was nitrogen (23 kcal/mol) > hexane (21 kcal/mol) > hexadecane (17 kcal/mol). Suppressed activation energy is indicative of diffusion resistance.

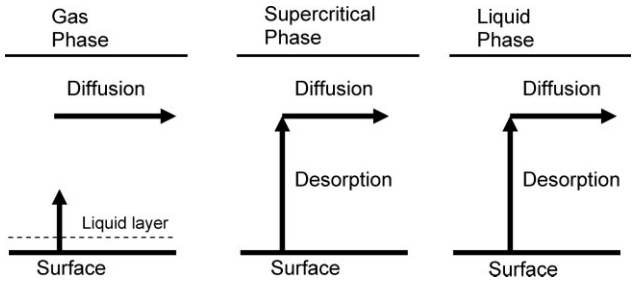

Figure 5. Model of overall diffusion of the products in three reaction phases.[24]

Nevertheless, Huang and Roberts[35] have shown that activity in the SCF-FTS over a cobalt catalyst is higher than in the gas-phase FTS despite the fact that mass transport and product bulk diffusion rates are higher in the gas phase than in the supercritical phase. Their steady state data (after 20 h time-on-stream (TOS) for SCF and 30 h TOS for gas phase) showed that operating FTS in Sc-hexane yields higher CO conversions (ca. 70%) relative to the gas-phase FTS (ca. 60%) (as shown in Figure 6). In addition, their findings show that steady-state operation was achieved more rapidly under the SCF-FTS than in the gas-phase FTS. They attributed these results to the higher solubility and in situ extractability of the SCF, resulting in suppressed wax accumulation in the catalyst pores. Moreover, the interfacial transport resistance that occurs due to condensed product on the catalyst surface under gas-phase FTS operation can be reduced under supercritical-phase operation by the solubility-driven removal of the heavy hydrocarbons.[35] By using a simulated wax, Yokota et al.[59] were able to simulate the extraction process of heavy wax from inside the catalyst pores for three different modes of operation (gas-phase, liquid-phase, and supercritical FTS). Their findings show that wax can be easily and quickly extracted from the catalyst pores in both the

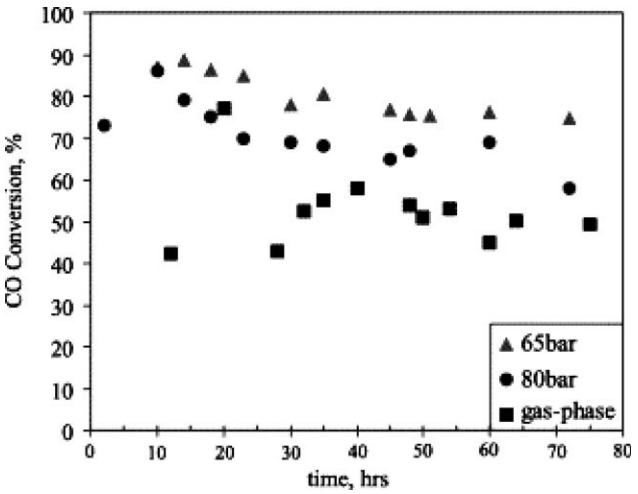

Figure 6. CO conversion in gas-phase and supercritical-phase FTS (temperature: 250°C; pressure (SCF phase): 65, 80 bar; syngas partial pressure (gas phase and SCF phase): 20 bar; hexane flow rate: 1 ml/min; syngas flow rate: 50 sccm/$g_{catalyst}$; syngas ratio (H_2/CO): 2:1).[35]

supercritical phase and the liquid-phase operation (up to 80% extraction within 1 h), while little was extracted during gas-phase operation. Similar results over a precipitated iron catalyst were reported by Bukur et al.[45] They have shown that catalyst activity in the supercritical mode of operation was slightly higher than that during conventional FTS in the fixed-bed reactor (FBR). They attributed this result to higher diffusivities of reactants in supercritical fluids relative to the conventional mode of operation (pores filled with liquid hydrocarbon wax).

Effects of SCF-FTS on Methane and Carbon Dioxide Selectivity. SCF-FTS (relative to gas phase FTS) has consistently been shown to suppress methane formation,[27,30,35,36,47,52,60] though it had no effect in one case[45] where propane was used as the SCF solvent (high reduced temperature). It has been pointed out[15] that hot spots can lead to elevated methane selectivity (among other problems). The dense supercritical media has been shown to give better axial thermal uniformity than gas phase FTS,[35,37,59] which suggests better general thermal uniformity and reduced hot spots. Davis' group (Jacobs et al.[27]) and Roberts' group (Durham et al.[30]) have demonstrated that SCF-FTS shifts the oxygen removal from carbon dioxide toward water on cobalt and iron catalysts, respectively. While this should allow for greater carbon efficiency, it requires the formation of more hydrogen, which would come at the cost of converting more CO to CO_2 during gasification.

Additionally, Fujimoto's group (Yan et al.[60]) showed that SCF-FTS gives a more uniform syngas concentration within individual catalyst pellets. Diffusion resistances in gas phase operation result in higher H_2/CO ratios within catalyst pellet, and these elevated syngas ratios increase the methane selectivity.

Effects of SCF-FTS on Olefin Selectivity. Reports have generally shown significant improvement in alpha-olefin selectivity during the SCF-FTS compared to either the gas-phase or the liquid-phase operation.[32,37,39,47,52] More precisely, a mild suppression[34,59] or no effect[35] is seen in going from gas phase-FTS to SCF-FTS on olefin selectivity at low carbon number while SFC-FTS is consistently seen to enhance the olefin selectivity with increasing carbon number.[27,30,32–34] 2-olefin selectivities have been shown to be lower in SC-FTS.[34] This is in keeping with the supercritical media's capacity for extracting products from catalyst pores, preventing secondary reactions (hydrogenation and double bond isomerization). α-olefins are considered as one of the most valuable chemicals from FTS since they can be used in number of industrial and consumer products. Most FTS kinetic models (for both cobalt and iron catalyst systems) consider α-olefins as the primary product of the synthesis process. Fan and Fujimoto[37] have reported a comparison of the olefin contents of hydrocarbon products in each reaction-phase on a Ru/Al_2O_3 catalyst. Their findings showed that the olefin content in the products decreased in each reaction-phase with an increase in carbon number. The decrease in the olefin content with the increasing carbon number could be attributed to the increase in the hydrogenation rate relative to diffusion rate with increasing carbon number (as a result of longer residence time on the catalyst surface derived from the slower diffusion rate of these olefins).[37] They attributed improvement in olefin content in the SCF-FTS relative to the gas phase-FTS (as shown in Figure 7) to the enhanced extraction of primary products (α-olefin) from the catalyst pores in the supercritical phase prior to secondary reactions (e.g., hydrogenation, isomerization, etc.). It is noteworthy to mention here that their findings are in agreement with the previous reports of Bukur et al. on a precipitated iron catalyst (see Figure 8).[32,34] Their explanation to the higher olefin content in SCF-FTS vs. that in the gas phase is that during gas phase FTS high molecular weight products (C_{8+} hydrocarbons) leave the reactor preferentially in the liquid state, and their residence time is longer than that of either the gas phase products, or the products formed during supercritical FTS. Also, diffusivities of high molecular weight α-olefins in the liquid hydrocarbon wax that fills the catalyst pores during gas phase operation are significantly lower than the corresponding diffusivities in the supercritical propane, and hence the pore residence time of these products is longer during the gas phase FTS. Longer residence time in the reactor and/or catalyst pores increases the probability for secondary readsorption of α-olefins, and results in secondary formation of *n*-paraffins and 2-olefins.[32] Also, desorption rates of heavy α-olefins are higher in Sc-propane than in liquid filled

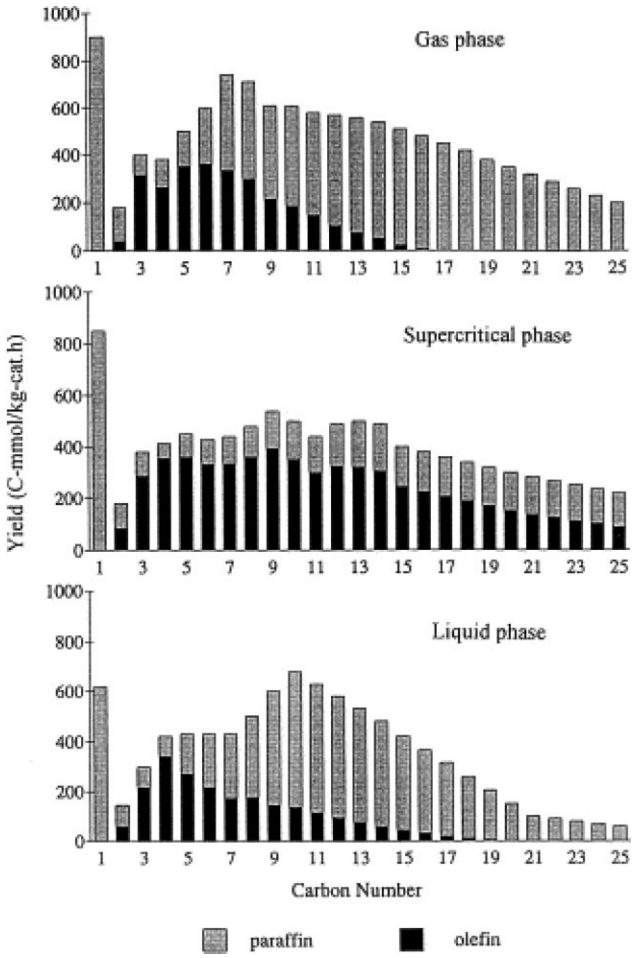

Figure 7. Olefin distribution in hydrocarbon products of FTS reactions in various phases over Ru/Al_2O_3 catalyst.[37]

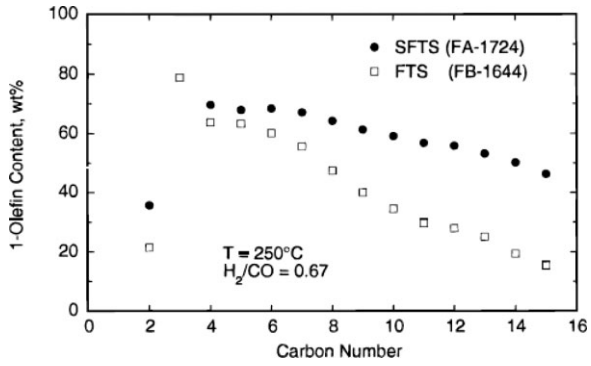

Figure 8. Comparison of α-olefin content during conventional FTS (run FB-1644) and SFTS (run FA-1724) at 250°C (H_2/CO) 0.67; syngas conversions 82% (FB-1644) and 76% (FA-1724).[32]

pores during conventional FTS,[28] which results in higher selectivity of primary products.

Later, Bukur et al.[45] showed that at similar syngas conversions olefin selectivity during the liquid-phase FTS is lower than that in the gas-phase FTS, which in turn is lower than that in the SCF-FTS. This may be attributed to a longer residence time of the liquid products in the stirred tank slurry reactor (STSR) compared to the fixed bed reactor (FBR). In the STSR the liquid products accumulate in the reactor, and are periodically withdrawn from it every 48–100 h, whereas in the downflow FBR they leave the reactor continuously by gravity. Also, the differences in mixing patterns (perfect mixing in the STSR vs. plug flow in the FBR) may have had some effect on olefin selectivities. Huang and Roberts[35] have also observed significantly higher olefin selectivity in SCF-FTS than in the gas-phase process for products with carbon numbers greater than 7 (as shown in Figure 9). They found that olefin content decreases with an increase in carbon number at a much slower rate in the supercritical phase than in the gas phase FTS resulting in significantly higher olefin production.

Catalyst Deactivation and Life Time in SCF-FTS. Deactivation of catalysts during FTS has been attributed to many causes including the poisoning or blocking of catalytic active sites by products or carbonaceous species,[61] the partial reoxidation of the catalyst (especially cobalt-based catalysts) at the surface by water or the oxygen produced by CO dissociation,[24] sintering/agglomeration of the active material.[14] Effective in situ extraction of heavy hydrocarbon products from the catalyst pores resulted in an ability to maintain high catalyst activity in a SCF mixture of pentane and hexane at 54.5 bar.[27] A high degree of catalyst stability has been observed when conducting FTS in supercritical media, even after long TOS.[34,48] Lang et al.[34] demonstrated that operating FTS under Sc-propane (the results of which are shown in Figure 10) over a precipitated iron catalyst stabilized the catalyst activity for a relatively long period of time (120 h) with higher CO conversion and H_2/CO usage ratio than for the conventional gas phase reaction (included as a base-line condition in Figure 10 for comparison). They also showed that returning to the gas-phase reaction after SCF-FTS operation sustained the catalyst activity for more than 250 h in total.

Elbashir et al.[48] reported the performance of three cobalt-based catalytic systems (high surface area 15% Co/SiO_2, low surface area 15% Co/SiO_2, and 15% Co/Al_2O_3) in both

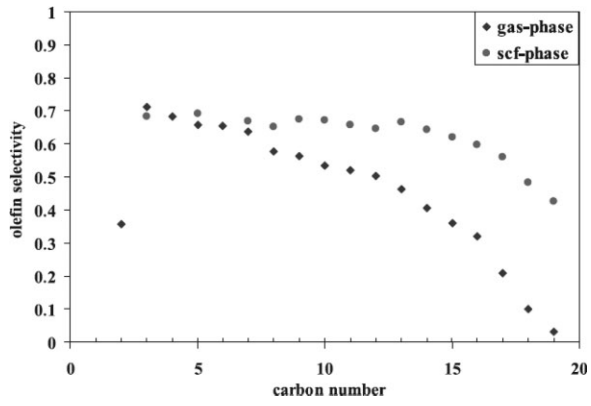

Figure 9. Olefins selectivity in supercritical-phase and gas-phase FTS (temperature: 250°C; pressure (SCF Phase): 80 bar; syngas partial pressure (gas phase and supercritical phase): 20 bar; hexane flow rate: 1 ml/min; syngas flow rate: 50 sccm/g catalyst; syngas ratio (H_2/CO): 2:1).[35]

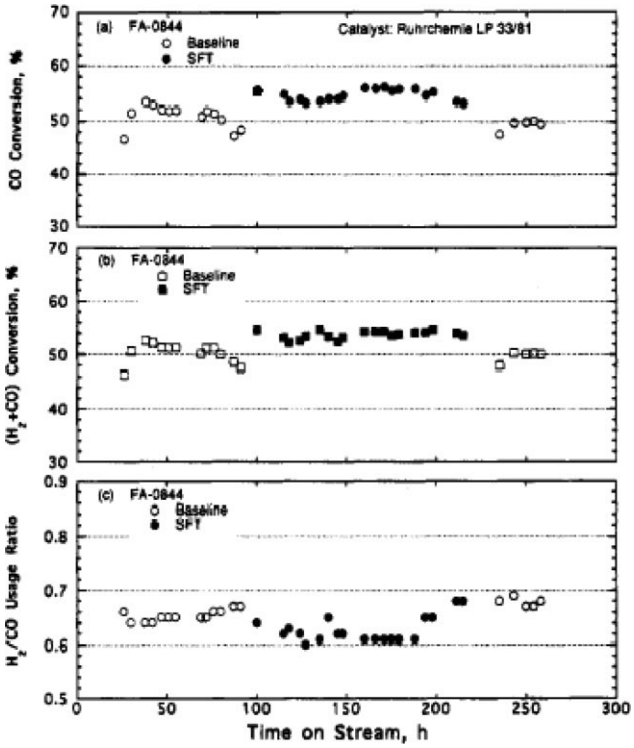

Figure 10. Variations in CO conversion (a), (H_2 + CO) conversion (b), and H_2/CO usage ratio (c) with time on stream in run FA-3143.

Open symbols (baseline conditions): P_{H2+CO} = 1.48 MPa, 250°C, 2 L(NTP)/(h*g of cat), H_2/CO = 0.67; solid symbols: P = 7 MPa ($P_{H2/CO}$= 1.48 MPa, P_{N2} = 5.52 MPa).[34]

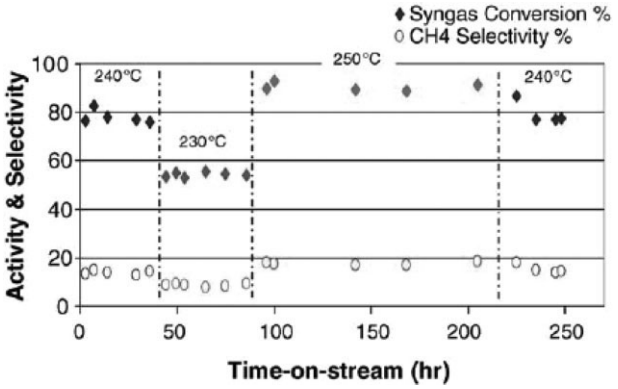

Figure 11. Stability of the 15% Co/Al_2O_3 catalyst activity (syngas conversion (%)) and selectivity (CH_4 selectivity (%)) with TOS in SCH-FTS at different reaction conditions (240°C and 60 bar; 230°C and 60 bar; 250°C and 65 bar; and 240°C and 60 bar).

P_{syngas} = 20 bar, syngas flow rate 50 sccm/g_{cat}, and hexane/syngas molar ratio is 3.[48]

conventional gas-phase and supercritical hexane FTS. They characterized the catalysts using several analytical instruments to measure surface characteristics and to determine the electronic states of the cobalt catalyst (Co^0, CoO, Co_3O_4, Co^{2+}) before and after reaction. Their XRD and magnetic characterizations of the used catalysts reveal that in situ reducibility of the Co_3O_4 to hcp-Co^0 or fcc-Co^0 took place during the FTS reaction. However, minimal in situ reduction was observed in the case of gas phase FTS, whereby significant changes in the reduced cobalt electronic state and support (alumina, and silica) phase were detected under SCF-FTS conditions. Figures 11 and 12 show examples of stability tests on the alumina-supported catalyst (15% Co/Al_2O_3) under different reaction conditions in SCF-FTS and gas-phase FTS at relatively long TOS. Under Sc-hexane conditions (Figure 11), the initial catalyst stability test was conducted at 240°C and 60 bar for 48 h TOS. During this time, the catalyst showed good stability in syngas conversion and in CH_4 selectivity (Relatively high methane selectivity was reported in Figures 11 and 12, potentially because the catalyst was not reduced prior to the reaction. However, this does not negate the validity of the comparison between GP-FTS and SCF-FTS operation.). Both the catalyst activity and its methane selectivity were found to change with temperature and upon returning to the initial conditions no significant changes in either syngas conversions or CH_4 selectivities were observed in SCF-FTS. On the other hand, in the gas phase FTS study (see Figure 12), the stability test revealed a significant drop (≈20%) from the initial catalyst activity over 180 h on stream with a corresponding drop in methane selectivity. Their[48] XRD and magnetic characterizations of the used catalysts show that in situ reducibility of the cobalt oxide takes place during the FTS reaction in both gas phase-FTS and SCF-FTS conditions. However, under SCF-FTS conditions the in situ reduction of Co_3O_4 gave active crystal-lines of hcp and fcc-Co^0 that were found to be very stable for a long TOS (15 days). As a result, the activity and selectivity of the catalyst in the SCF hexane medium was found to be more stable and recoverable than that under gas phase-FTS conditions.

Roberts' group[39] has also shown that SCF-FTS maintains the catalyst's surface area and pore volume better than gas phase FTS operation. Irankhah et al.[51] confirmed this observation, showing that SCF-FTS gives less of a loss of BET surface area, catalyst pore volume, and average pore diameter than gas phase FTS. In addition to promoting the formation of methane, hot spots enhance the formation of coke precursors, which can lead to catalyst fouling.[14] Consequently, this mode of deactivation in gas phase-FTS should be decreased in SCF-FTS operation.

Product distribution and kinetics studies of SCF-FTS

Hydrocarbon Product Distribution and Control of Selectivity in SCF-FTS. The Anderson-Schultz-Flory (ASF) model is a common model used to describe the chain growth mechanism in FTS and is developed based on Flory's[62] pioneering studies on the fundamental nature of polymerization. The basic structure of the ASF model was developed through a series of extensive studies[63–65] that led to the current, well-known ASF product distribution model. This model assumes that the polymerization process in FTS initiates on the surface of the catalyst by a monomer that contains one carbon atom, while chain growth takes place by the addition of one monomer at a time.

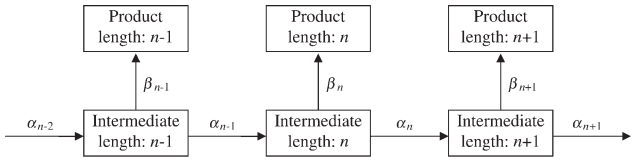

α_n is the probability of an intermediate of length n propagating to a length of $n + 1$; β_n is the probability of an intermediate of length n terminating to a length of n; $\alpha_n + \beta_n = 1$ (by definition).

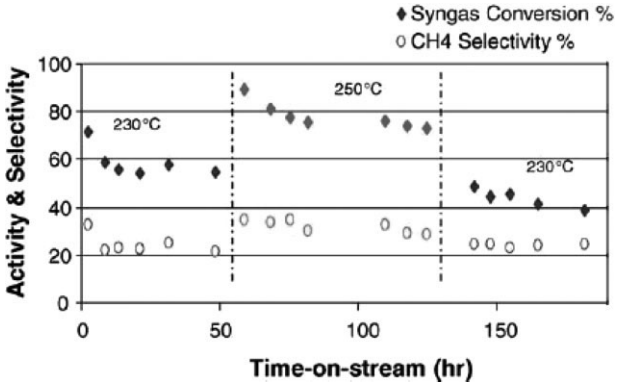

Figure 12. Stability of the 15% Co/Al_2O_3 catalyst activity (syngas conversion (%)) and selectivity (CH_4 selectivity (%)) with TOS in gas phase-FTS at different reaction conditions (230°C and 20 bar; 250°C and 20 bar; and 230°C and 20 bar).

P_{syngas} = 20 bar, syngas flow rate 50 sccm/g_{cat}.[48]

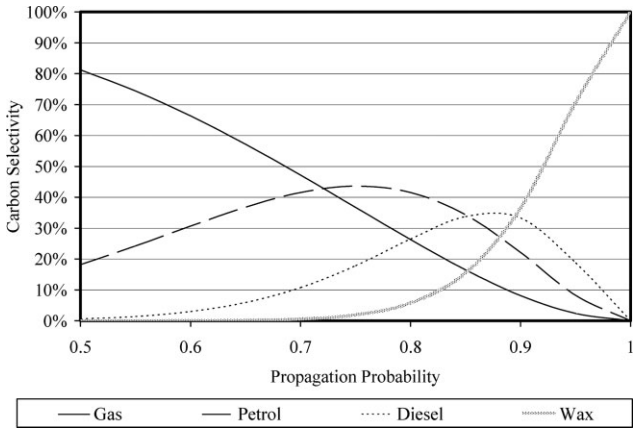

Figure 13. Fuel fraction selectivity as a function of propagation probability, α-value.

The second assumption in the ASF model is that the propagation probability (α) is a constant ($\alpha_1 = \alpha_2 = \alpha_3 = \alpha_n = \alpha$). These assumptions lead to the following equation[66]:

$$\Phi_n/\Phi_x = \alpha^{n-x}$$

where $\Phi_n \equiv$ mole fraction of length n. Additionally, approximating Φ_n as (W_n/n) leads to:

$$W_n = n\alpha^{n-1}(1-\alpha)^2 \tag{1}$$

$$\ln\left(\frac{W_n}{n}\right) = n\ln\alpha + \ln\left(\frac{(1-\alpha)^2}{\alpha}\right) \tag{2}$$

W_n represents the weight fraction of all hydrocarbon products with carbon number n, and α is chain-growth probability which is the rate of growth divided by the sum of growth and termination rates. According to this ASF model, a plot of $\ln(W_n/n)$ vs. n (as in Eq. 2) should yield a straight line for all hydrocarbon products whereby the α-value can be determined from the slope of that line. According to Eq. 2, a higher α-value yields a heavier hydrocarbon weight product distribution.

Under industrial HTFT conditions, a propagation probability of 0.7[14] is typical. For LTFT, a propagation probability of 0.95 is typical.[24] The ASF model dictates that there is a maximum achievable selectivity of both the gasoline and diesel fractions possible without subsequent upgrading. A typical fuel fractions selectivity as function of α-value is shown in Figure 13.

The two most common deviations from the ASF model involve C1 and C2 selectivity, where actual C1 production is greater than the ASF model predicts and actual C2 production is often lower than the ASF model predicts.[31] A third deviation type is the double alpha distribution. In this distribution, the low carbon number products show a low propagation probability and the high carbon number products show a high propagation probability, with the transition often occurring around C12.[67] A fourth type of ASF distribution is the sigmoid distribution, in which the product distribution has a shoulder (especially in the middle distillate range).[68]

Numerous studies have reported deviations from this standard product distribution in FTS yielding different curvatures for the relationship between $\ln(W_n/n)$ vs. n.[69] Many researchers have targeted such deviations as a means to control the product distribution in FTS to maximize the production of hydrocarbons within specific carbon number ranges (e.g., C_5–C_{11} for gasoline fraction, C_{12}–C_{19} for diesel fraction, or higher carbons for heavy wax range). Successful deviation from the standard ASF distribution would represent a breakthrough in FTS technology that would allow for higher selectivity toward the most desired products such as transportation fuels (e.g., diesel fuels).

Many reaction pathways and kinetic models have been developed to explain observed deviations from the standard ASF model. Mass transfer limitations inside the catalyst pores due to the condensation of heavy hydrocarbons was one of the reasons suggested for enhanced α-olefin (primary products) readsorption thereby increasing the production of heavy hydrocarbons.[70] Huff and Satterfield also suggested a model that proposes two catalytic sites with two different growth factors (for iron promoted catalysts) that yield a positive deviation from the standard ASF model.[71] Pore size effects (molecular sieve effects)[72] and concentration gradients as well as temperature gradients in fixed bed reactors[73] were also suggested as causes for non ASF distributions. In a series of studies, Puskas and his coworkers argue that multiplicity in the chain growth probability is the reason for positive deviations from the ASF model.[74–76] In addition, deviations from the ASF model have also been attributed to experimental artifacts, nonsteady-state operation, and transient holdup of higher molecular weight products in the oil phase surrounding the catalyst.[77,78]

Several studies reported an enhancement in chain growth probability and an increase of selectivity toward high value α-olefins in SCF-FTS compared to conventional gas-phase FTS and liquid-phase FTS. Higher productivity of α-olefins, a primary product in the FTS chain growth process, indicates suppression of secondary reactions such as hydrogenation to paraffins, isomerization and oxygenations under SCF conditions. Examples of the enhanced productivity of α-olefins in SCF-FTS have been discussed in the previous section. In SCF-FTS deviations from the ASF product distributions were reported in several studies. Tsubaki et al.[44] reported an interesting non-ASF product distribution in Sc-pentane at a reaction temperature of 200°C over a silica supported cobalt catalyst. The authors reported a hydrocarbon product distribution where the formation rate of hydrocarbons from C_7 to C_{28} was nearly independent of the carbon number, with an α-value higher than 0.96 (see Figure 14). They suggested that the supercritical phase provided an increased ability of the formed olefins (C_nH_{2n}) to readsorb on active sites and initiate new chain-growth processes, increasing the formation rate of heavy hydrocarbons.[44] To support this interesting experimental data, a chain growth mechanism has to be developed to explain the manner by which C_8 and C_{26} behave equally in initiating new chains, promoting heavier hydrocarbon production with a similar rate of formation. The concept of α-olefins incorporation is not a new one.[79] It has been shown that in the presence of carbon monoxide and

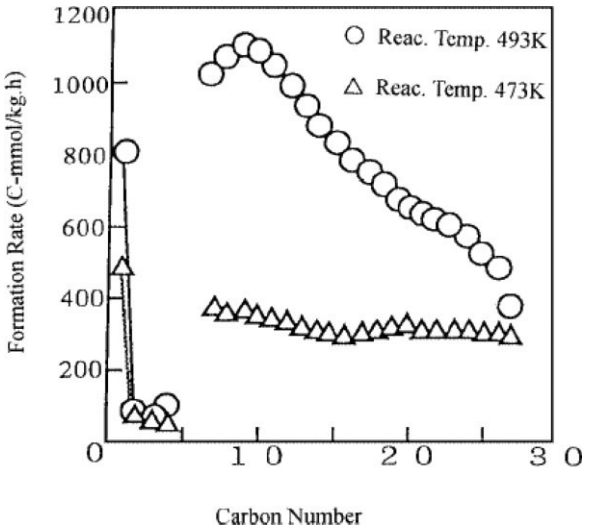

Figure 14. Anti-ASF hydrocarbon distribution in FTS reactions with supercritical-phase *n*-pentane.

Co/SiO_2 = 40/100 (wt); *P* (total) = 45 bar; *P* ($CO + H_2$) = 10 bar; *P* (*n*-pentane) = 35 bar; CO/H_2 = 1/2; *W/F* ($CO + H_2$) = 9 g/mol h 1.[44]

hydrogen, ethylene can react on a cobalt-based catalyst to form large quantities of higher hydrocarbons and oxygen-containing compounds. Several other studies have also shown that α-olefins can incorporate in the chain-growth process and behave similarly to the FTS building blocks by either initiating a new chain or becoming a part of a growing one, specifically for cobalt catalysts.[80–82]

However, another study[27] used mixed supercritical solvents (55% hexane-45% pentane) with an alumina supported cobalt catalyst at 220°C and over a wide range of pressures (from 23 bar to 54.5 bar). This study indicated that hydrocarbon distributions beyond C_{10} closely followed the ASF distribution (see Figure 15). No information about the light hydrocarbon (C_1–C_9) distribution was presented in this study. Similarly, Lang et al.[34] reported that FTS operation at

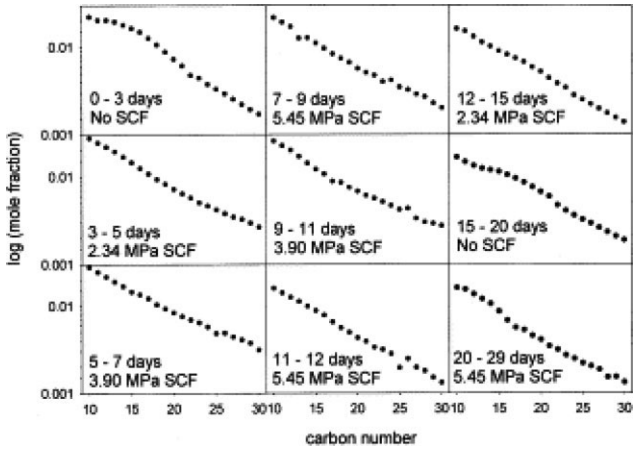

Figure 15. Product distribution for C_{10}-C_{30} Carbon number products during various operating periods.[27]

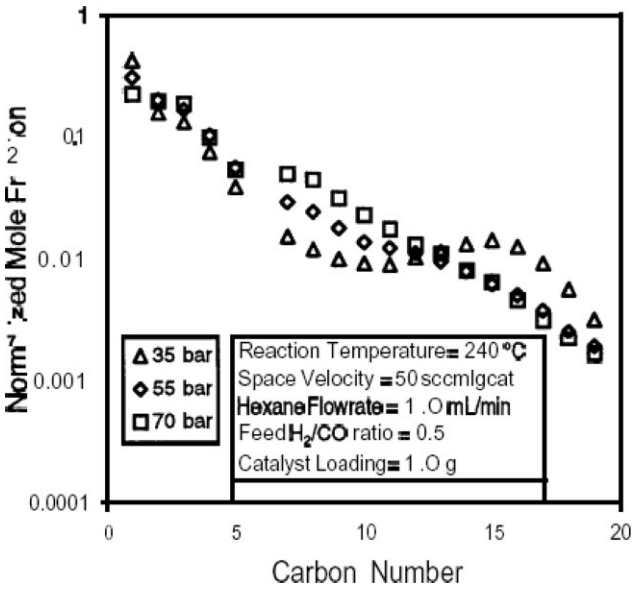

Figure 16. Pressure tuning effects on steady-state ASF product distribution (α-value).[29]

supercritical conditions over a precipitated iron catalyst did not have marked effect on the lumped hydrocarbon product distribution. On the other hand, Bochniak and Subramaniam[29] reported non-ASF distributions in Sc-hexane FTS on Ruhrchemie iron catalyst at a temperature of 240°C by varying the pressure from 35 bar (gas-like density) to 70 bar (liquid-like density). Their product distributions, shown in Figure 16, illustrate the existence of a shoulder in the carbon fractions from C_5 to C_{10} that decreased with increasing pressure; however, there were no significant changes in the light product distribution (C_1–C_4) with pressure. This phenomenon was reported to disappear after 80 h time-on-stream. Furthermore, they[29] attributed the enhanced chain growth probability in the Sc-hexane medium to the enhanced extraction of heavier olefins in the liquid-like medium prior to any secondary reactions taking place. Meanwhile, at high pressure (70 bar) they suggested that the diffusion rate of α-olefins decreased significantly, resulting in regular ASF distributions.

Elbashir and Roberts[47] reported significant deviation from the standard ASF model within SCH-FTS in near-critical and supercritical conditions (controlled by tuning the reaction temperature and/or pressure) over an alumina supported cobalt catalyst. The degree of deviation from the ASF model was found to vary from near-critical to supercritical and from liquid-like density to gas-like density. They suggested that the hydrocarbon product distribution in SCH-FTS should be represented by more than one chain growth probability for different ranges of hydrocarbons, as shown in Figure 17. Very high chain growth probability (α-value ≈ 0.95) was observed within the middle distillate hydrocarbons (i.e., C_5–C_{15}) as shown in Figure 17. This phenomenon was attributed to the enhanced α-olefin incorporation in the chain growth process and a model for the reaction network and chain growth pathway was proposed accordingly.[47] Their model assumes that only α-olefins have the capability of readsorbing and incorporating into the chain growth process. As seen

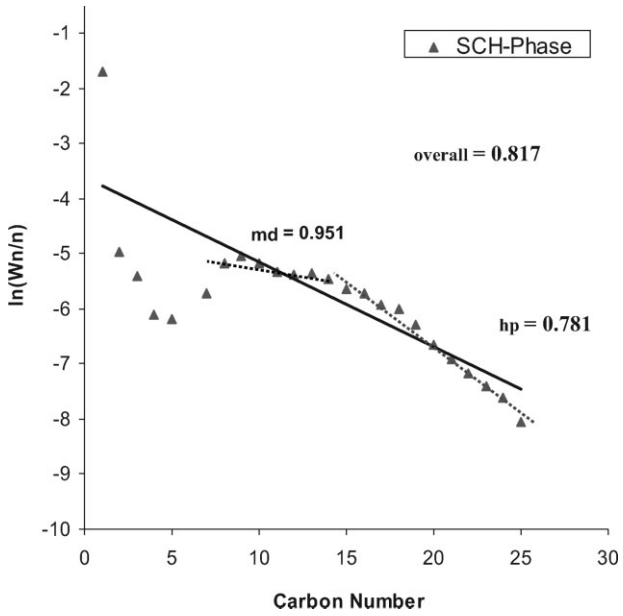

Figure 17. Hydrocarbon product distribution obtained from SCH-FTS.

$\alpha_{overall}$ represents the slope of the solid line and was calculated from the standard ASF model; α_{lp}, α_{md}, α_{hp} represent the chain growth probability of the light hydrocarbons, middle distillates, and heavy hydrocarbons, respectively.[47]

in Figure 18b, the first point in the curve represents the methane selectivity (which was referred to as methanation). The light hydrocarbon (C_2–C_5) selectivity region is defined as the regular olefin incorporation range that could participate in the propagation process and thus their concentrations in the final products may be decreased relative to what estimated by the standard ASF model. Based on this analysis they[47] introduced the *enhanced olefin incorporation range* as a unique contribution of the influence of the near-critical and supercritical solvent (hexane) on the FTS chain growth process. The incorporation of olefins from C_7 to C_b (where b represents the carbon number where deviation from linear ASF model no longer exists and the product distributions beyond that carbon number follow the ASF model; see Figure 18) is attributed to the enhanced solubility of primary products in the single phase near-critical or supercritical fluid, which affects the adsorption/desorption equilibrium of those species.

To verify the possibility of olefin readsorption in SCF-FTS, Shi et al.[46] conducted a ^{14}C-labeled study over alumina supported cobalt catalyst using a mixture of pentane/hexane as the supercritical solvent in a fixed bed reactor. They chose middle distillate olefins such as decene, tetradecene, and nonadecene as the ^{14}C probe compounds to investigate the readsorption probability of these olefins in the chain growth process. They found that the molar radioactivity of the incorporated compounds decreases with increasing molecular size, indicating the presence of some accumulated products under these reaction conditions. The ASF plot of the incorporated compound in the ^{14}C-labeled decene gave a similar α-value to that without the addition of decene, which they suggest indicates that the added middle size olefin cannot produce hydrocarbons that result in an anti-ASF product distribution. While these results are not in agreement with the previous

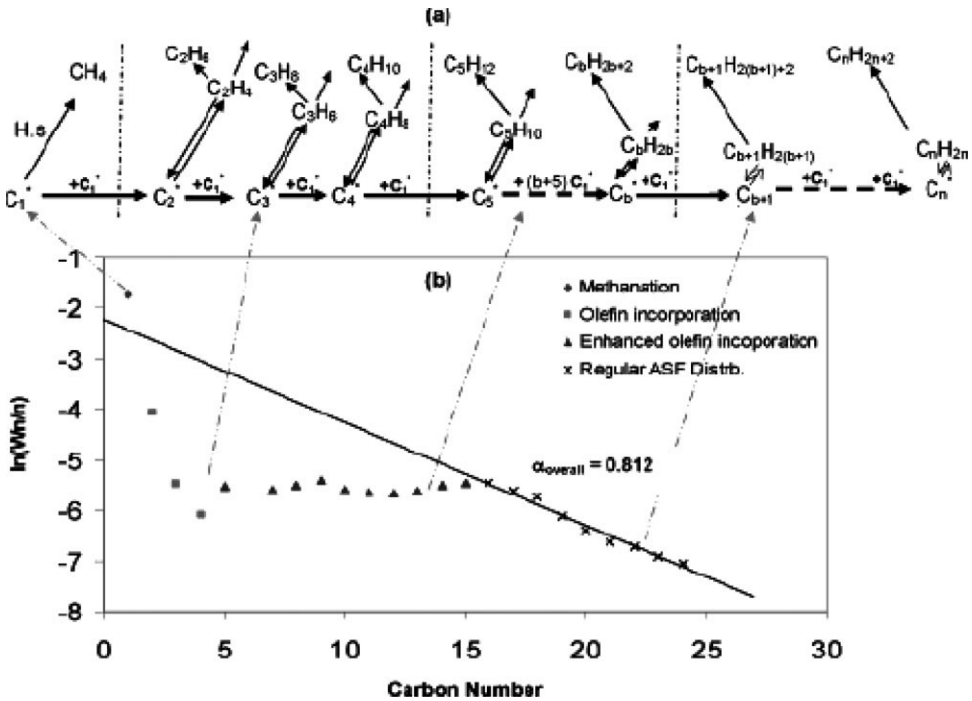

Figure 18. (a) Description of the chain growth process in the enhanced olefin incorporation model in SCH-FTS starting with methanation and ending with the heaviest hydrocarbon detected under the specific reaction conditions; (b) typical product distribution curve in SCH-FTS including all regions defined in the chain growth process above.[47]

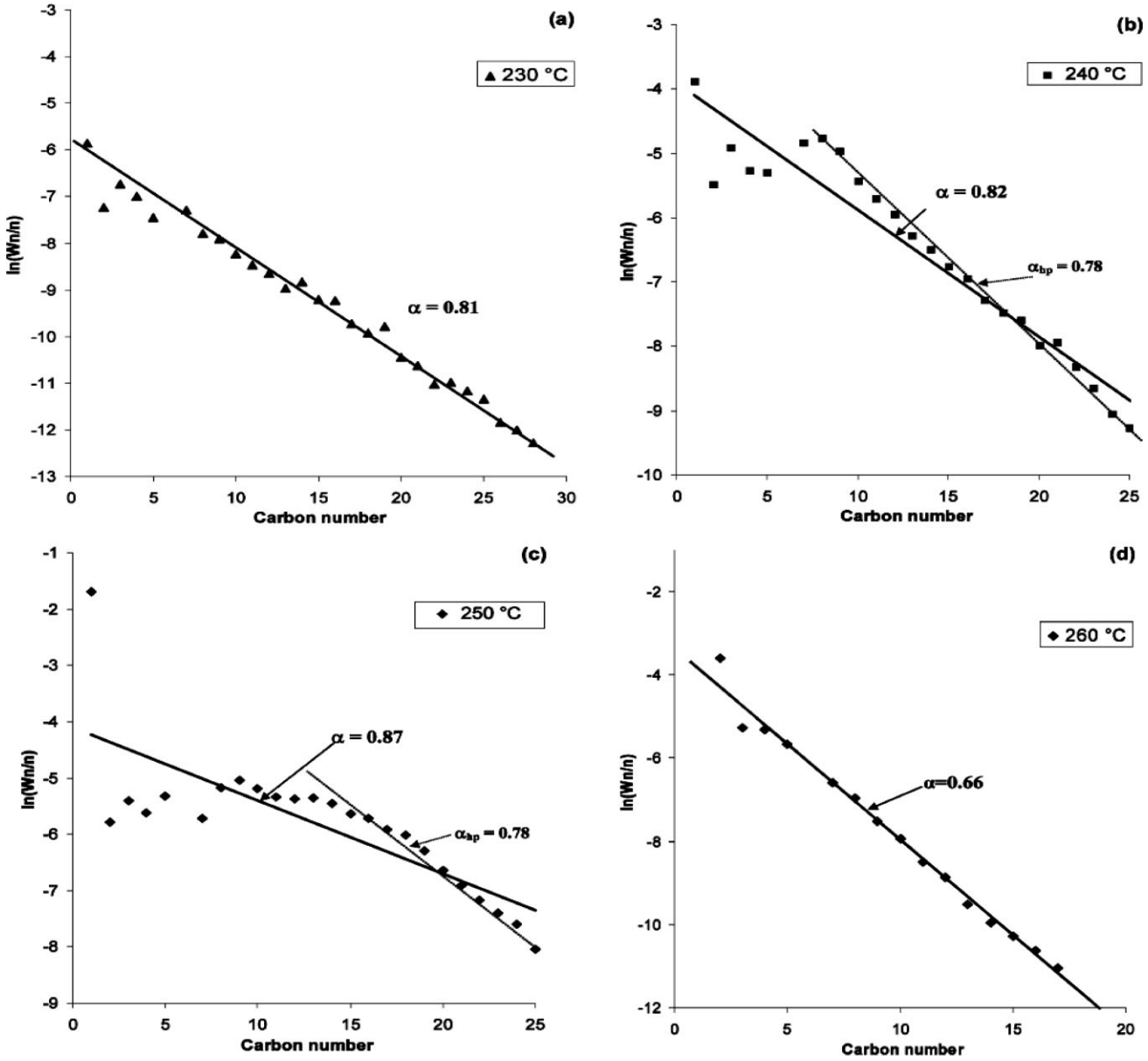

Figure 19. Hydrocarbon product distribution from SCH-FTS at 65 bar and (a) T_1 = 230°C, (b) T_2 = 240°C, (c) T_3 = 250°C, and (d) T_4 = 260°C.

Catalyst: 15% Co/Al_2O_3, reaction conditions: syngas 50 sccm/g_{cat} flow rates, hexane: 1.0 mL/min, and H_2/CO feed ratio of 2. α represents the overall chain growth probability for all hydrocarbon products. α_{hp} represents the chain growth probability of the heavy products.[47]

reports of Tsubaki et al.[44] and the proposed *enhanced-olefin incorporation* model of Elbashir and Roberts,[47] Shi et al.[46] make it clear in their conclusion that their reaction conditions, such temperature, pressure, and supercritical media are different from those of Fujimoto group[46] reported data.

The importance of temperature and pressure as well as other reaction conditions on the hydrocarbon product distribution in SCF-FTS has been explored by Elbashir and Roberts.[47] Figure 19a–d show the changes in the ASF product distribution as function of reaction temperature as it changes from 230 to 260°C. It is noteworthy to mention here that at 230°C the reaction mixture exists as a compressed liquid phase as evidenced by the experimental measurement of the critical properties of the reaction mixture[47] (see T_1 in Figure 4). On the other extreme, operation at 260°C results in a reaction mixture that is well within the supercritical region (i.e., the temperature is well above the mixture critical temperature) under these conditions[47] (see T_4 in Figure 4). The overall hydrocarbon distribution closely followed the ASF model at 230°C with a chain growth probability α-value of 0.81 (which agrees with Shi et al.[46] ASF plots). Increasing the temperature to 240°C, whereby the reaction mixture is maintained near the critical point, the overall chain growth probability is maintained at 0.82 as shown in Figure 19b. The product distribution in Figure 19b follows closely the ASF model in the middle distillate and heavy hydrocarbon

range whereas marked deviations are observed in the light hydrocarbon range. As shown in Figure 19b, the deviations extend to C_8 (i.e., deviations are in the range of C_2–C_8). Surprisingly, upon increasing the temperature to 250°C (well within the supercritical region), no substantial drop in the chain growth probability of heavy hydrocarbons (α_{hp}-value of 0.78) was observed despite the increase in the reaction temperature while the overall α-value increased to 0.87. In addition, the range of deviation from the ASF model extended up to C_{14} (i.e., deviation range from C_2 to C_{14}) as shown in Figure 19c (which agrees with Tsubaki et al.[44] ASF plots). A further increase in temperature (T_4 of 260°C), resulting in a gas-like density, produced a drastic drop in the chain growth probability ($\alpha_{overall} = 0.66$) as shown in Figure 19d. The overall product distribution of hydrocarbons up to C_{20} closely followed the ASF model, while only very slight deviation in C_2 selectivity is seen in the product distribution at this elevated temperature (which agrees with Shi et al.[46] ASF plots).

One conclusion that can be drawn from this is that supercritical FTS operation is not sufficient in itself to produce these deviations from the standard ASF product distributions. Rather, it is a combined result of proper selection of a number of process parameters including temperature and pressure that affect both the thermophysical characteristics of the fluid medium as well as the system kinetics. Because of the complexity of the supercritical-phase FTS operation, understanding the reaction kinetics and proposing chain growth pathways requires the following; (1) understanding of the phase behavior of the solvent/reactant and the solvent/reactant/product mixture, (2) detailed product distributions from C_1 up to heavier hydrocarbon products under the specified reaction conditions, and (3) an understanding of the interrelation of the phase behavior of the reaction mixture and the FTS performance (e.g., product distributions and consumption rates of the reactants).

Kinetics and Modeling of Reaction Pathways in Supercritical Phase FTS. Few studies reported mechanistic and kinetic modeling of SCF-FTS.[29,40,83] Fan et al.[40] suggested the following empirical power rate law for SCH-FTS over Ru catalysts of different pore diameter and pore size:

$$r = kP_{H_2}^{x}P_{CO}^{y} \tag{3}$$

where k is the rate constant and x and y are the exponential constants. They referred to previous FTS kinetic models[84,85] that suggested that the rate of an FTS reaction on ruthenium catalysts is first order in H_2. As a result, they were able to calculate the apparent rate constant for each catalyst (of different pore diameter and size) and defined the catalyst effectiveness factor as the ratio between the rate of reaction in supercritical fluid to that in gas phase reaction.

Bochniak and Subramaniam[29] studied the effects of pressure tuning on syngas conversion and catalyst effectiveness factor. In order for them to explain the increase in syngas conversion with reactor pressure in a supercritical fluid medium, they correlated the effective rate constants (ηks) with the pressure. The expression for an effective rate constant (mol/(min bar $g_{catalyst}$)) was derived by assuming a plug-flow reactor and that the syngas conversion is pseudo first order reaction in H_2 (they referred to Anderson's[86] kinetic model for syngas conversions below 60%).

The effective rate constant is estimated using the following simplified form of the stoichiometric equation, which implies dominant olefin formation and rapid water-gas shift activity.

$$H_2 + 2CO \rightarrow \frac{1}{n}(CH_2) + CO_2 \tag{4}$$

Upon assuming plug-flow behavior and also considering syngas conversion as pseudo first-order in hydrogen (A) partial pressure, Bochniak and Subramaniam[29] were able to derive the following expression for the effective rate constant.

$$\eta k = \left(\frac{F_{S0}}{P_T F_{S0} W}\right)(-F_0 \ln(1 - x_A) + 2F_{A0}\{\ln(1 - x_A) + x_A\}) \tag{5}$$

The partial pressure of H_2 (P_A) is related to the total pressure P_T as in the equation below:

$$P_A = \left(\frac{F_A}{F_T}\right)P_T = \left(\frac{F_{A_0}(1 - x_A)}{F_0 - 2x_A F_{A_0}}\right)P_T \tag{6}$$

where F_A is the molar flow rate of species A (hydrogen), mol/min; F_{A0} is the inlet molar flow rate of A (hydrogen), mol/min; F_0 is total inlet molar flow rate, mol/min; F_{S0} is inlet molar flow rate of S (syngas), mol/min; F_T is the total molar flow rate, mol/min; P_A is the partial pressure of species A (hydrogen), bar; P_T is the total operating pressure, bar; k is the intrinsic rate constant, mol/(min bar g catalyst), and x_A is the conversion of species A (hydrogen); and W is the weight of catalyst, g.

The calculated effective rate constant (ηk) as well as the effectiveness factor η were found to increase with the increase of pressure in the system. This was attributed to the alleviation of pore diffusion limitations (viz., maintenance of wider pore channels) resulting from enhanced extraction of heavier hydrocarbons from the catalyst pores by the liquid-like densities, yet significantly better-than-liquid diffusivities of *n*-hexane.[29]

Both of the previously suggested rate equations for the SCF-FTS rely on gas-phase and liquid-phase kinetic models, which result in very simplified rate equation formulas. Elbashir and Roberts[83] suggested a reaction network for SCF-FTS that takes into account the role of enhanced α-olefin incorporation in the chain growth process under SCF operation (see Figure 20). The model assumes that operating FTS in SCF medium promotes the in situ extraction of heavy products from the catalyst pores and as a result accessibility to active sites increases. Those vacant sites (due to the enhanced extraction) were assumed to promote both adsorption of CO and H_2 and incorporation of α-olefins in the chain growth process. The kinetics model and the reaction pathway were derived from the surface reaction kinetic model as outlined in Elbashir and Roberts[83] using developed kinetics model for cobalt catalysts.[87–89] The proposed reaction pathway shown in Figure 20 assumes that the characteristics of Co catalyst site very much control the initial stages of the synthesis (stages 1–3), implying the supercritical

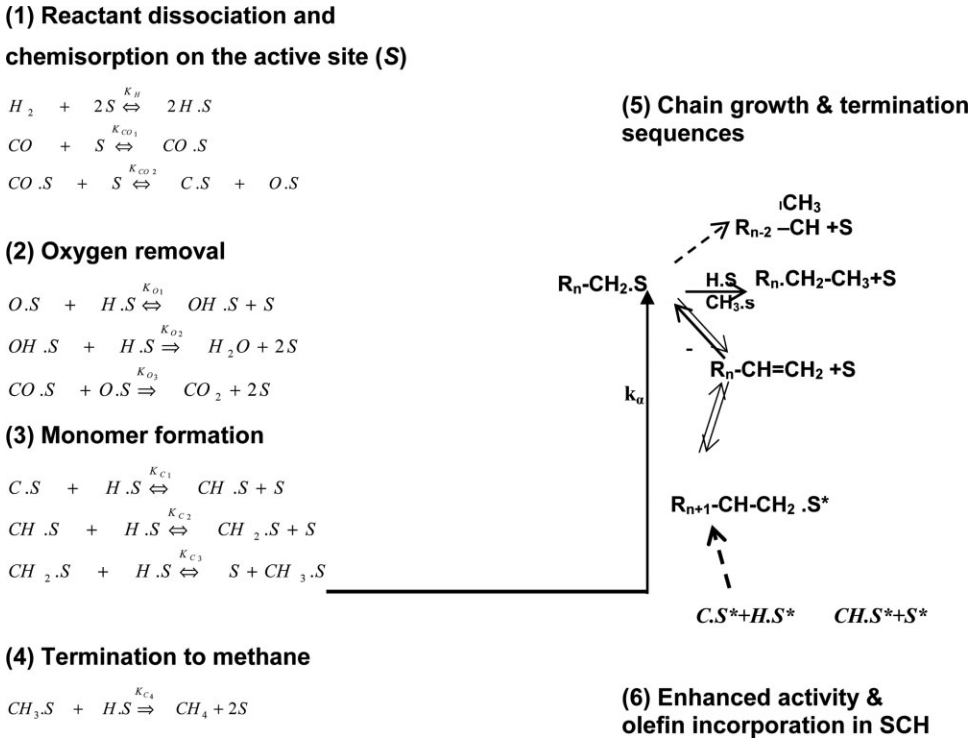

Figure 20. FTS reaction network including the enhanced activity and olefin incorporation sites.[83]

solvent has the least influence at these stages. The reaction rate equations were then derived by using the simplified assumptions of Sarup and Wojcichowski[90] to yield the following rate expression for CO consumption:

$$-r_{CO} = \frac{kP_{CO}^{1/2}P_{H_2}^{1/2}}{\left[1 + K_1P_{H_2}^{1/2} + (K_2 + K_3)P_{CO}^{1/2} + K_4P_{CO}\right]^2} \quad (7)$$

This model was found to be in a good agreement with the experimental results obtained from the gas-phase FTS, though, it poorly predicted the behavior under Sc-hexanes FTS. The authors[83] suggested improving the kinetic model to predict SCH-FTS behavior by including thermodynamic nonidealities into the rate expression, and quantifying the influence of modified active site (evacuated ones, *S**). This site (*S**) is assumed to promote both adsorption of the reacting molecules (CO and H_2) and at the same time facilities the participation of primary products (α-olefins) into the chain growth process. It is also assumed that *S** would have a higher coverage of active carbon than the regular site, *S*; and therefore, it suppresses methane formation.[83] In addition they assumed that the effective reaction order of higher hydrocarbon formation on *S** is higher than the methane formation since the monomer involved on this site is likely a desorbed olefin close to the active site. Even though[83] suggested contribution of *S** (as shown in Figure 20) in enhancing both activity and chain growth probability in SCF-FTS are in agreement with their experimental data[47] there is still need for developing quantitative model capable of predicting FTS reaction behavior in near critical and supercritical phase over wide range of operating conditions.

In a recent study, Irankhah et al.[91] derived the rate equations for the supercritical phase FTS reactions for a cobalt-ruthenium catalyst in supercritical hexane. The reaction rate constants were determined from the Langmuir-Hinshelwood-Hougen-Watson model for the overall rates CO conversion and CH_4 formation. The calculated activation energy for their cobalt-ruthenium catalyst l was found to be in agreement with previously reported values[40,83] of cobalt-based catalysts.

Challenges and prospects in commercializing SCF-FTS technology

Very recently, Elbashir et al.[92] reported preliminary investigations on the optimization of the design of separation processes (for light hydrocarbons) and a solvent recovery unit in a simulated FTS pilot-plant scale operating under SCF conditions. The separation unit is simulated by a flash distillation column that operates at different combinations of temperature/pressure depending on reactor operating conditions. The design aimed at utilizing pressure and temperature drop in the separation process to separate the reaction media from the reaction products. Success in this direction would represent a major advantage for the SCF-FTS process over conventional FTS technologies since it has always been challenged by the high cost of compression/pumping and other costs associated with high pressure equipment. The findings shows that by fine tuning temperature and pressure in the flash distillation column it is possible to recover the

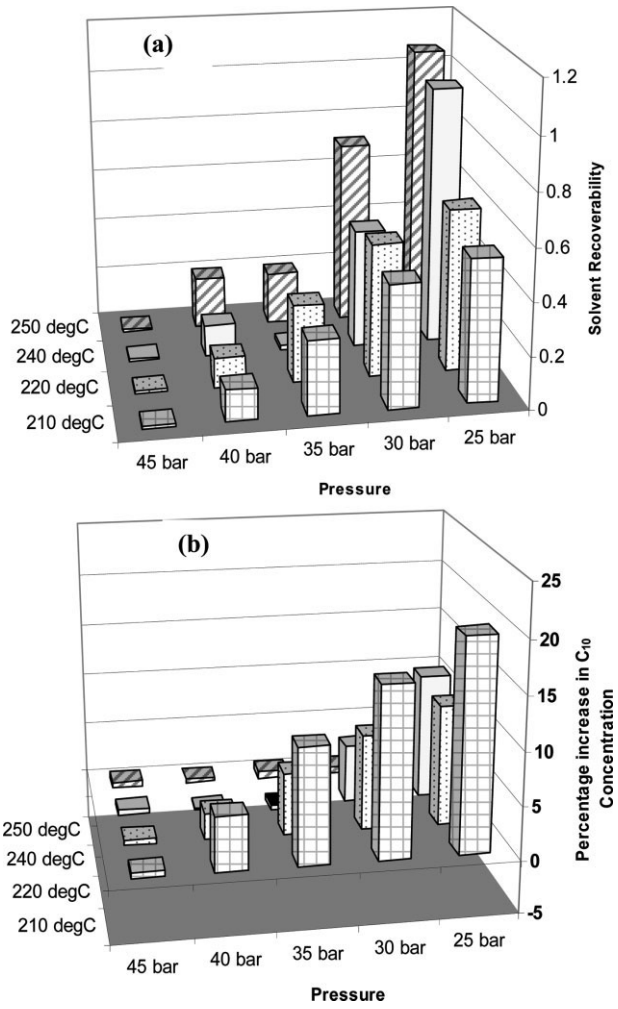

Figure 21. (a) Solvent recoverability as function of pressure and temperature in the flash distillation column and (b) percentage increase in C_{10+} concentration as a result of solvent recovery.[92]

supercritical solvent and the light hydrocarbon fractions without affecting the other hydrocarbon products of interest.

The ability to separate the supercritical solvent (considered in this case as a hydrocarbon mixture of C_5–C_7 with hexanes representing the major component of the mixture) from a hydrocarbon mixture was simulated as a flash distillation column using the property method NRTL-RK in ASPEN.[92] Solvent recoverability was calculated as the normalized difference between the concentration of solvent (C_5–C_7) at reactor outlet and the concentration at the top of the flash distillation column (collected as vapor phase). Figure 21a shows the effect of both temperature and pressure on solvent recoverability as pressure dropped in steps from 45 bar (refers to pressure inside reactor bed) to 25 bar (refers to pressure in the flash distillation column). The data shows that solvent recoverability increases as pressure decreases at fixed temperature, while better recoverability is obtained at the higher temperature. More importantly, Figure 21b illustrates that the concentrations of middle distillate and heavy hydrocarbon fractions (C_{10+}) collected at the bottom of the flash distillation column increased as pressure decreased from 45 bar to 25 bar for all studied temperatures. This finding supports the basic concept that the light hydrocarbon fractions, including the supercritical solvent, can be recovered without significantly affecting the other hydrocarbon products of interest.

Experimental demonstration of supercritical solvent recyclability from FTS reaction mixture has been demonstrated by Fujimoto's team.[93] They have successfully designed and tested a recycle reactor system for supercritical FTS. Their new reactor system has these characteristics: (1) integration of supercritical FTS reactions, natural separation of produced wax from liquid phase, and recycle of the solvent and (2) natural recycle of solvent driven by self-gravity. Under their reaction conditions, they found that average CO conversion at the steady state and with SCF recycle is lower that the CO conversion without recycle (45% vs. 58%). However, they found no significant difference between the overall hydrocarbon product distribution for the process with and without SCF recycling. Their XRD result indicates that solvent recycle did not have any effect on the Co crystal structure of catalyst.[93]

Despite the numerous literature contributions, reports, and patents on FTS catalysts, reaction chemistry, reaction pathways, and reaction kinetics, very few studies have reported reactor design alternatives to the conventional aforementioned FTS technologies. deDeug et al.[94] in their review of the conventional FTS technologies concluded that the selection of a proper FTS reactor technology for a given GTL plant was always a nonoptimal compromise between the advantages and disadvantages of each existing reactor technology. Industry urgently needs the development of an advanced FTS technology to overcome the limitations of the existing, conventional FTS technology platforms as was well described in the presentation of Dr. Ben Jager at the 2003 spring meeting of the American Institute of Chemical Engineering in New Orleans.[95] Dr. Jager concluded his presentation by making the following statements (1) GTL technology is at early stage of development; (2) there is an incentive for improved FTS technology; and (3) new FTS reactors are early on the learning curve.

Conclusions and Remarks

It is noteworthy to mention that most of the successful commercial GTL technologies require tremendous financial and operational support which is available only to large corporations; while small companies are still seeking the development of profitable small-scale GTL plants with fewer technical complications. Supercritical fluids are unique reaction media leverage certain advantages of the current commercial technologies (slurry reactor and multitubular reactor) while at the same time overcoming several of their major limitations. Supercritical solvents are a unique media for chemical reactions because they offer single phase operation with densities that are sufficient to afford substantial dissolution power, while also providing diffusivities that are higher than normal liquids and viscosities that are lower than their liquid counterparts. These properties result in significant enhancements of mass transfer and/or heat transfer and can result in significant reductions in the size of the reactor bed required.

The use of hydrocarbons for catalyst regeneration and for cooling purposes is not a new idea, it was applied in several commercial FTS processes[96] including Shell's SMDS reactor in Bintulu, Malaysia.[97] It was reported that a C_5 or C_6 hydrocarbon injection protocol for cooling is used to improve productivity by reducing heat transfer limitations. While, as covered in this review, a great deal of research has been done in simulation and at the bench-top scale, there are still gaps in the research that need to be filled. A more thorough understanding of the transport and thermodynamic behavior of the SCF-FTS reaction environment would offer great benefits in understanding and modeling reactor performance. Of particular importance is the possibility of allowing the reaction to be carried out in a lower number of larger tubes (which would simplify the reactor design and reduce the reactor's cost). This design factor could be effectively studied on a pilot scale.

Despite the numerous studies that have examined FTS in SCF media, the development of this technology has not yet moved beyond the lab scale. Elbashir et al.[92] outlined the following steps toward developing a pilot plant FTS reactor technology based on supercritical fluids operation:

- Synthesis of novel reactor configurations that use pressure drop as a means of separating and recycling unreacted syngas and supercritical solvent to the reactor.
- Simultaneous evaluation and optimization of reaction parameters (temperature, pressure, solvent, etc.) on both the phase behavior of the reaction mixture and the underpinning reaction kinetics.
- Optimization of the overall process design using advanced process integration techniques coupled with dynamic control systems.
- Evaluation of the performance of the synthesized systems via process simulation.
- Experimental testing of developed pathways and comparison with theoretical studies.

In conclusion, we recommend developing design strategies for future SCF-FTS reactor systems that have features similar to the approach proposed by Krishna and Sie.[98] Optimizing the design of a SCF-FTS reactor would require multidisciplinary expertise since the introduction of the tunable supercritical solvent shifts the problem from a classical catalytic reaction engineering process to one combined with a thermophysical puzzle. As a result, the parametric studies needed for the design includes thermodynamics and phase behavior of nonideal reaction mixtures; reaction kinetics of the synthesis process under these nonideal conditions, detailed studies on catalyst performance, stability, and characteristics; process control studies; and energy integration and process optimization for individual units as well as for the overall process.[92] Future research should focus on developing such strategies and frameworks that facilitate pilot plant and commercial reactor design for SCF-FTS.

Having said all this, while there are certainly aspects of SCF-FTS that it would be ideal to have resolved prior to scaling up to pilot plant, there is also much to learn that can best be studied at the pilot scale. For a research group to operate SCF-FTS at that scale would offer extraordinary benefits to understanding this field. This is the next major step in SCF-FTS and we feel the field is ready for someone to take it.

Literature Cited

1. Cagniard de LaTour C. Supercritical fluids. *Ann Chim Phys*. 1822; 21:127–132.
2. McHugh MA, Krukonis VJ. *Supercritical Fluid Extraction*, 2nd ed. Boston: Butterworth-Heinemann, 1994.
3. Johnson KP, Penninger JML, editors. Supercritical fluid science and technology. *Developed From a Symposium at the American Institute of Chemical Engineers Annual Meeting*, Washington, DC, November 27–December 2, 1988:550.
4. Baiker A. Supercritical fluids in heterogeneous catalysis. *Chem Rev*. 1999;99:453–474.
5. Subramaniam B. Enhancing the stability of porous catalysts with supercritical reaction media. *Appl Catal A: Gen*. 2001;212:199–213.
6. Hyde JR, Licence P, Carter D, Poliakoff M. Continuous catalytic reactions in supercritical fluids. *Appl Catal A: Gen*. 2001;222:119–131.
7. Guisnet M, Magnoux P. Deactivation by coking of zeolite catalysts. Prevention of deactivation. Optimal conditions for regeneration. *Catal Today*. 1997;36:477–483.
8. Freemantle M. Continuous SCF reactor. *Chem Eng News*. 1997; 79:30.
9. Savage PE, Gopalan S, Mizan TI, Martino CJ, Brock EE. Reactions at supercritical conditions: applications and fundamentals. *AIChE J*. 1995;41:1723–1778.
10. Satio S. Research activities on supercritical fluid science and technology in Japan—a review. *J Supercrit Fluids*. 1995;8:177–204.
11. Subramaniam B. Supercritical phase catalysis—heterogeneous. In: Horvath IT, editor. *Encyclopedia of Catalysis*. American Chemical Society, Washington, DC, 2003.
12. Jessop GJ, Leitner W. *Chemical Synthesis Using Supercritical Fluids*. Weinheim: Wiley-VCH, 1999.
13. Seki T, Grunwaldt J, Baiker R. Heterogeneous catalytic hydrogenation in supercritical fluids: potential and limitations. *Ind Eng Chem Res*. 2008;47:4561–4585.
14. Dry ME. Present and future applications of the Fischer-Tropsch process. *Appl Catal A: Gen*. 2004;276:1.
15. Van Der Laan GP, Beenackers AACM. Kinetics and selectivity of the Fischer-Tropsch synthesis: a literature review. *Catal Rev*. 1999; 41:255.
16. Wilhelm DJ, Simbeck DR, Karp AD, Dickenson RL. Syngas production for gas-to-liquids applications: technologies, issues, and outlooks. *Fuel Proc Technol*. 2001;71:139.
17. Aasberg-Peterson K, Christensen TS, Dybkjaer I, Sehested J, Ostberg M, Coertzen RM, Keyser MJ, Steynberg AP. Synthesis gas production for FT synthesis. In: Steynberg AP, Dry ME, editors. *Studies in Surface Science and Catalysis*. Amsterdam: Elsevier Science, 2004: Chapter 4.
18. Dancuart LP, de Haan R, de Klerk A. Processing of primary Fischer Tropsch products. In: Steynberg A, Dry M, editors. *Studies in Surface Science and Catalysis, Vol. 152: Fischer-Tropsch Technology*. Amsterdam: Elsevier Science, 2004:482–532.
19. Dry ME. The Fischer-Tropsch process: 1950–2000. *Catal Today*. 2002;71:227.
20. Steynberg AP, Espinoza RL, Jager B, Vosloo AC. High temperature Fischer-Tropsch synthesis in commercial practice. *Appl Catal A: Gen*. 1999;186:41.
21. Espinoza RL, Steynberg AP, Jager B, Vosloo AC. Low temperature Fischer-Tropsch synthesis from a sasol perspective. *Appl Catal A: Gen*. 1999;186:413.
22. Steynberg AP, Dry ME, Davis BH, Breman BB. Fischer-Tropsch reactors. In: Steynberg AP, Dry ME, editors. *Studies in Surface Science and Catalysis*. Amsterdam: Elsevier Science, 2004; *Chapter 2*:152.
23. Dry ME. Practical and theoretical aspects of the catalytic Fischer-Tropsch process. *Appl Catal A: Gen*. 1996;138:319.
24. Jager B, Espinoza R. Advances in low temperature Fischer-Tropsch synthesis. *Catal Today*. 1995;23:17–28.
25. Bukur DB, Sivaraj C. Supported iron catalysts for slurry phase Fischer-Tropsch synthesis. *Appl. Catal. A: Gen*. 2002;231:201.
26. Tijmensen MJA, Faaij APC, Hamelinck CN, van Hardeveld MRM. Exploration of the possibilities for production of Fischer Tropsch liquids and power via biomass gasification. *Biomass Bioenergy* 2002;23:129–152.

27. Jacobs G, Chaudhari K, Sparks D, Zhang Y, Shi B, Spicer R, Das TK, Li J, Davis BH. Fischer-Tropsch synthesis: supercritical conversion using a Co/Al_2O_3 catalyst in a fixed bed reactor. *Fuel*. 2003; 82:1251–1260.
28. Yokota K, Hanakata Y, Fujimoto K. Supercritical phase Fischer-Tropsch synthesis. *Chem Eng Sci*. 1990;45:2743–2749.
29. Bochniak DJ, Subramaniam B. Fischer-Tropsch synthesis in near-critical n-hexane: pressure-tuning effects. *AIChE J*. 1998;44:1889–1896.
30. Durham E, Zhang S, Roberts CB. Supercritical reactivation of Fischer Tropsch catalysts. AIChE Annual Meeting (2008): Presentation 678d. In: Durham E Bordawekar M, Roberts CB, editors. *Effects of Super-Critical Fluid Extraction on the Activity and Selectivity of Fischer Tropsch Catalysts. Preprints of Symposia*. Washington, DC: Division of Fuel Chemistry, American Chemical Society, 2007.
31. Claeys M, van Steen M. Basic studies. In: Steynberg A, Dry M, editors. *Studies in Surface Science and Catalysis, Vol. 152: Fischer-Tropsch Technology*. Amsterdam: Elsevier Science, 2004:601–680.
32. Bukur DB, Lang X, Akgeman A, Feng Z. Effect of process conditions on olefin selectivity during conventional and supercritical Fischer-Tropsch synthesis. *Ind Eng Chem Res*. 1997;36:2580–2587.
33. Yokota K, Hanakata Y, Fujimoto K. Supercritical-phase Fischer-Tropsch synthesis reaction. III. Extraction capability of supercritical fluids. *Fuel*. 1991;70:989–994.
34. Lang X, Akgeman A, Bukur DB, Steady state F-T synthesis in supercritical propane. *Ind Eng Chem Res*. 1995;34:72–77.
35. Huang X, Roberts CB. Selective Fischer-Tropsch synthesis over an Al2O3 supported cobalt catalyst in supercritical hexane. *Fuel Proc Tech*. 2003;83:81–99.
36. Yokota K, Fujimoto K. Supercritical phase Fischer-Tropsch synthesis reaction. *Fuel*. 1989;68:255–256.
37. Fan L, Fujimoto K. Fischer-Tropsch synthesis in supercritical fluids: characteristics and application. *Appl Catal A: Gen*. 1999;186:343–354.
38. Li J, Jacobs G, Das T, Davis BH. Fischer-Tropsch synthesis: effect of water on the catalytic properties of a ruthenium promoted Co/TiO_2 catalyst. *Appl Catal A: Gen*. 2002;233:255–262.
39. Huang X, Elbashir NO, Roberts CB. Supercritical solvent effects on hydrocarbon product distributions in Fischer-Tropsch synthesis over an alumina supported cobalt catalyst. *Ind Eng Chem Res*. 2004;43:6369–6381.
40. Fan L, Yokota K, Fujimoto K. Supercritical phase Fischer-Tropsch synthesis: catalyst pore-size effect. *AIChE J*. 1992;38:1639.
41. Sun S, Tsubaki N, Fujimoto K. The reaction performances and characterization of Fischer-Tropsch synthesis Co/SiO_2 catalysts prepared from mixed cobalt salts. *Appl Catal A: Gen*. 2000;202:121–131.
42. Fan L, Yoshii K, Yan S, Zhou J, Fujimoto K. Supercritical-phase process for selective synthesis of wax from syngas: catalyst and process development. *Catal Today*. 1997;36:295–304.
43. Tsubaki N, Fujimoto K. Product control in Fischer-Tropsch synthesis. *Fuel Proc Technol*. 2000;62:173–186.
44. Tsubaki N, Yoshii K, Fujimoto K. Anti-ASF distribution of Fischer-Tropsch hydrocarbons in supercritical-phase reactions. *J Catal*. 2002;207:371–375.
45. Bukur DB, Xiaos L, Nowicki L. Comparative study of an iron Fischer-Tropsch catalyst performance in stirred tank slurry and fixed-bed reactors. *Ind Eng Chem Res*. 2005;44:6038–6044.
46. Shi B, Jacobs G, Sparks D, Davis B. Fischer-Tropsch synthesis: 14C labeled 1-alkene conversion using supercritical conditions with $Co/A1_2O_3$. *Fuel*. 2005;84:1093–1098.
47. Elbashir NO, Roberts CB. Enhanced incorporation of α-olefins in the Fischer-Tropsch synthesis chain-growth process over an alumina supported cobalt catalyst in near-critical and supercritical hexane medium. *Ind Eng Chem Res*. 2005;44:505–521.
48. Elbashir NO, Dutta P, Manivannan A, Seehra MS, Roberts CB. Impact of cobalt-based catalyst characteristics on the performance of conventional gas-phase and supercritical-phase Fischer Tropsch synthesis. *Appl Catal A: Gen*. 2005;285:169.
49. Zhou J, Yan S, Gao Z, Fan L. Supercritical phase process for selective synthesis of heavier hydrocarbons from syngas on cobalt catalysts. *ACS Div Petrol Chem Prep*. 2002;47:154–157.
50. Yan S, Zhang Z, Zhou J, Deng DJ, Fan K. Study on diffusion of syngas in supercritical fluid and heavy paraffinic F-T product. *Fudan Xuebao Ziran Kexueban*. 2002;41:325–329 (Journal in Chinese).
51. Irankhah A, Haghtalab A. Fischer-Tropsch synthesis over Co-Ru/α-Al_2O_3 catalyst in supercritical media. *Chem Eng Technol*. 2008; 31:525–536.
52. Tang H, Liu H, Yang X, Li Y. Supercritical phase Fischer-Tropsch synthesis reaction over highly active fused iron catalysts at low temperature. *Cuihua Xuebao*. 2008;29:174–178 (Journal in Chinese).
53. Gao L, Hou Z, Zhang H, He J, Liu Z, Zhang X, Han B. Critical parameters of hexane + carbon monoxide + hydrogen and hexane + methanol + carbon monoxide + hydrogen mixtures in the hexane-rich region. *J Chem Eng Data*. 2001;46:1635–1637.
54. Joyce PC, Gordon J, Thies MC. Vapor-liquid equilibria for the hexane + tetracosane and hexane + hexatriacontane systems at elevated temperatures and pressures. *J Chem Eng Data*. 2000;45:424–427.
55. Joyce PC, Leggett BE, Thies MC. Vapor-liquid equilibrium for model Fischer-Tropsch waxes (hexadecane, 1-hexadecene, and 1-hexadecanol) in supercritical hexane. *Fluid Phase Equilb*. 1999;158–160:723–731.
56. Polishuk I, Statevab RP, Wisniakc J, Segurad H. Simultaneous prediction of the critical and sub-critical phase behavior in mixtures using equations of state. IV. Mixtures of chained n-alkanes. *Chem Eng Sci*. 2004;59:633–643.
57. Linghu W, Li X, Asami K, Fujimoto K. Supercritical phase Fischer-Tropsch synthesis over cobalt catalyst. *Fuel Proc Technol*. 2004; 85:1121–1138.
58. Linghu W, Li X, Fujimoto K. Supercritical and near-critical Fischer-Tropsch synthesis: effects of solvents. *J Fuel Chem Technol*. 2007; 35:51–56.
59. Yokota K, Fujimoto K. Supercritical-phase Fischer-Tropsch synthesis reaction. II. The effective diffusion of reactant and products in the supercritical-phase reaction. *Ind Eng Chem Res*. 1991;30:95.
60. Yan S, Fan L, Zhang Z, Zhou J, Fujimoto K. Supercritical-phase process for selective synthesis of heavy hydrocarbons from syngas on cobalt catalysts. *Appl Catal A: Gen*. 1998;171:247.
61. Anderson RB, Hall WK, Krieg A, Seligman B. Studies of the Fischer-Tropsch synthesis. V. Activities and surface areas of reduced and carburized cobalt catalysts. *J Am Chem Soc*. 1949;71:183–188.
62. Flory PJ. Molecular size distribution in linear condensation polymers. *J Am Chem Soc*. 1936;58:1877–1885.
63. Herington EFG. The Fischer-Tropsch synthesis considered as a polymerization reaction. *Chem Ind*. 1946:346–347.
64. Friedel RA, Anderson RB. Composition of synthetic liquid fuels. I. Product distribution and analysis of C5-C8 paraffin isomers from cobalt catalyst. *J Am Chem Soc*. 1950;72:1212–1215.
65. Henrici-Olive G, Olive S. The Fischer-Tropsch synthesis: molecular weight distribution of the primary products and reaction mechanism. *Angew Chem*. 1976;88:144–150.
66. Dry ME. The Fischer-Tropsch synthesis. In: Anderson JR, Boudart ME, editors. *Catalysis Science and Technology*, Vol. 1. New York: Springer, 1981:159–255.
67. Dry ME. Chemical concepts used for engineering purposes. In: Steynberg A, Dry M, editors. *Studies in Surface Science and Catalysis, Vol. 152: Fischer-Tropsch Technology*. Amsterdam: Elsevier Science, 2004:482–532.
68. Kuipers EW, Scheper C, Wilson JH, Vinkenburg IH, Oosterbeek H. Non-ASF product distributions due to secondary reactions during Fischer-Tropsch synthesis. *J Catal*. 1996;158:288–300.
69. Inoue M, Miyake T, Inui T. Simple criteria to differentiate a two-site model from a distributed-site model for Fischer-Tropsch synthesis. *J Catal*. 1987;105:266–269.
70. Madon RJ, Iglesia E, Reyes SC. Non-Flory product distributions in Fischer-Tropsch synthesis catalyzed by ruthenium, cobalt, and iron. *ACS Symp Ser (Selectivity in Catalysis)*. 1993;517:383–396.
71. Huff GA Jr, Satterfield CN. Evidence for two chain growth probabilities on iron catalysts in the Fischer-Tropsch synthesis. *J Catal*. 1984;85:370–379.
72. Iglesia E, Reyes SC, Soled SL. Reaction-transport selectivity models and the design of Fischer-Tropsch catalysts. *Chem. Ind*. 1993;51: 199–257.
73. Matsumoto DK, Satterfield CN. Effects of temperature and hydrogen/carbon monoxide ratio on carbon number product distribution from iron Fischer-Tropsch catalysts. *Energy Fuels*. 1989;3:249–254.
74. Puskas I, Hurlbut RS, Pauls RE. Telomerization model for cobalt-catalyzed Fischer-Tropsch products. *J Catal*. 1993;139:591–601; and references therein.

75. Hurlbut RS, Puskas I, Schumacher DJ. Fine details on selectivity and kinetics of the Fischer-Tropsch synthesis over cobalt catalysts by combination of quantitative gas chromatography and modeling. *Energy Fuels*. 1996;10:537–545.
76. Puskas I, Hurlbut RS. Comments about the causes of deviations from the Anderson-Schulz-Flory distribution of the Fischer-Tropsch reaction products. *Catal Today*. 2003;84:99–109.
77. Dictor RA, Bell AT. An explanation for deviations of Fischer-Tropsch products from a Schultz-Flory distribution. *Ind Eng Chem Proc DesDev*. 1983;22:678–681.
78. Davis B. Anderson Schulz Flory product distributions—can it be avoided for Fischer-Tropsch synthesis. In: *American Institute of Chemical Engineers (AIChE) 2003 Spring Meeting*, New Orleans, LA, 2003. (Related reference: Shi B, Keogh RA, Davis BH. Fischer-Tropsch synthesis: the formation of branched hydrocarbons in the Fe and Co catalyzed reaction. *J Mol Catal A: Chem*. 2005;234:85–97).
79. Smith DF, Hawk CO. The mechanism of the formation of higher hydrocarbons from water gas. *J Am Chem Soc*. 1930;52:3221–3232.
80. Snel R. The nature of hydrocarbons synthesis by means of hydrogenation of CO on iron-based catalysts. *J Mol Catal*. 1989;53:143–154.
81. Snel R, Espinoza RL. Secondary reactions of primary products of the Fischer-Tropsch synthesis. II. The role of propene. *J Mol Catal*. 1989;54:103–117.
82. Patzlaff J, Liu Y, Graffmann C, Gaube J. Studies on product distributions of iron and cobalt catalyzed Fischer-Tropsch synthesis. *Appl Catal A: Gen*. 1999;186:109–119.
83. Elbashir NO, Roberts CB. Reaction pathway and kinetic modeling of Fischer-Tropsch synthesis over an alumina supported cobalt catalysts in supercritical-hexane. *ACS Div Petr Chem Prep*. 2004;49:157–160.
84. Vannice MA. The catalytic synthesis of hydrocarbons from carbon monoxide and hydrogen. *Catal Rev Sci Eng*. 1976;14:153–191.
85. Karn FS, Shultz JF, Anderson RB. Hydrogenation of carbon monoxide and carbon dioxide on supported ruthenium catalysts at moderate pressures. *Ind Eng Chem Prod Res Dev*. 1965;4:265–269.
86. Anderson RB. *The Fischer-Tropsch Synthesis*. Academic Press: Orlando, FL, 1984.
87. Bell AT. Catalytic synthesis of hydrocarbons over Group VIII metals. Discussion of the reaction mechanism. *Catal Rev Sci Eng*. 1981;23:203–232.
88. Kellner CS, Bell AT. The kinetics and mechanisms of carbon monoxide hydrogenation over alumina-supported ruthenium. *J Catal*. 1981;70:418–432.
89. Uner DO. A sensible mechanism of alkali promotion in Fischer-Tropsch synthesis: adsorbate mobilities. *Ind Eng Chem Res*. 1998; 37:2239–2245.
90. Sarup B, Wojciechowski BW. Studies of the Fischer-Tropsch synthesis on a cobalt catalyst. I. Evaluation of product distribution parameters from experimental data. *Can J Chem Eng*. 1988;66:831–842.
91. Irankhah A, Haghtalab A, Farahani EV, Sadaghianizadeh K. Fischer-Tropsch reaction kinetics of cobalt catalyst in supercritical phase. *J Nat Gas Chem*. 2007;16:115–120.
92. Elbashir NO, Bao B, El-Halwagi MM. An Approach to the design of advanced Fischer-Tropsch reactor for operation in near-critical and supercritical phase media. In: Alfadalla HE, Reklaitis GV, El-Halwagi MM, editors. *Advances in Gas Processing: Proceedings of the 1st Annual Symposium on Gas Processing Symposium, Vol. 1*. Amsterdam: Elsevier, 2009:423–433.
93. Linghu W, Li X, Asami K, Fujimoto K. Process design and solvent recycle for the supercritical Fischer-Tropsch synthesis. *Energy Fuels*. 2006;20:7–10.
94. de Deug RM, Kapteijn F, Moulijn JA. Trends in Fischer-Tropsch reactor technology—opportunities for structured reactors. *Top Catal*. 2003;26:29–38.
95. Jager B. Fischer-Tropsch reactors. In: *American Institute of Chemical Engineering (AIChE) 2003 Spring Meeting*, New Orleans, 2003. (Related reference: Jager B, Van Berge P, Steynberg AP. Developments in Fischer-Tropsch technology and its application. *Stud Surf Sci Catal*. 2001;136:63–68).
96. Kolbel H, Ralek M. The Fischer-Tropsch synthesis in the liquid-phase. *Catal Rev*. 1980;21:225–274; and references therein.
97. World Fuels Today Editorial. Today's feature: supercritical phase' FT, CO_2-rich scheme highlights Japan SAE Conference Papers. *World Fuels TODAY*. 2003;July 3:1, 5–6.
98. Krishna R, Sie ST. Strategies for multiphase reactor selection. *Chem Eng Sci*. 1994;49:4029.

Manuscript received Feb. 24, 2009, and revision received Jun. 23, 2009.